

Chemical Technology
Division
Chemical Technology
Division

Corrosion Tests to Determine Temperature and pH Dependencies of the Dissolution Rates of Sodalite, Binder Glass, and Ceramic Waste Form

by S.-Y. Jeong, T. H. Fanning,
L. R. Morss, and W. L. Ebert



Argonne National Laboratory, Argonne, Illinois 60439
operated by The University of Chicago
for the United States Department of Energy under Contract W-31-109-Eng-38

Chemical Technology
Division
Chemical Technology
Division
Chemical Technology
Division
Chemical Technology
Division

Argonne National Laboratory, with facilities in the states of Illinois and Idaho, is owned by the United States Government and operated by The University of Chicago under the provisions of a contract with the Department of Energy.

DISCLAIMER

This report was prepared as an account of work sponsored by an agency of the United States Government. Neither the United States Government nor any agency thereof, nor The University of Chicago, nor any of their employees or officers, makes any warranty, express or implied, or assumes any legal liability or responsibility for the accuracy, completeness, or usefulness of any information, apparatus, product, or process disclosed, or represents that its use would not infringe privately owned rights. Reference herein to any specific commercial product, process, or service by trade name, trademark, manufacturer, or otherwise, does not necessarily constitute or imply its endorsement, recommendation, or favoring by the United States Government or any agency thereof. The views and opinions of document authors expressed herein do not necessarily state or reflect those of the United States Government or any agency thereof, Argonne National Laboratory, or The University of Chicago.

Available electronically at <http://www.doe.gov/bridge>

Available for a processing fee to U.S. Department of Energy and its contractors, in paper, from:

U.S. Department of Energy
Office of Scientific and Technical Information
P.O. Box 62
Oak Ridge, TN 37831-0062
phone: (865) 576-8401
fax: (865) 576-5728
email: reports@adonis.osti.gov

ANL-02/32

ARGONNE NATIONAL LABORATORY
9700 South Cass Avenue
Argonne, IL 60439

**CORROSION TESTS TO DETERMINE TEMPERATURE AND pH
DEPENDENCIES OF THE DISSOLUTION RATES OF SODALITE, BINDER GLASS,
AND CERAMIC WASTE FORM**

by

Seung-Young Jeong, Thomas H. Fanning*, Lester R. Morss, and William L. Ebert

Chemical Technology Division

*Reactor Analysis and Engineering Division

August 2002

CONTENTS

	<u>Page</u>
NOMENCLATURE	vii
ABSTRACT	1
1. INTRODUCTION	2
2. EXPERIMENTAL METHODS	4
2.1 STATIC TEST PROCEDURE	4
2.2 SINGLE-PASS FLOW-THROUGH TESTS	5
2.3 SAMPLE PREPARATION	7
2.4 BUFFER SOLUTION PREPARATION AND pH MEASUREMENT	8
3. CALCULATION OF TEMPERATURE AND pH DEPENDENCIES	9
3.1 STATIC TESTS IN TRADITIONAL BUFFER SOLUTIONS AT 40, 70, AND 90°C	9
3.2 STATIC TESTS IN NONCOMPLEXING BUFFER SOLUTIONS	9
3.3 MODEL PARAMETER VALUES	10
3.4 PREDICTABILITY OF RATE EXPRESSION	11
3.5 EFFECT OF CWF CONSOLIDATION METHOD	11
3.6 EFFECT OF GLASS COMPOSITION	12
3.7 STATIC TEST AND SINGLE-PASS FLOW-THROUGH TESTS WITH CSG GLASS	12
3.7.1 Static Test Method	12
3.7.2 Single-Pass Flow-Through Tests	13
3.7.3 Discussion	14
4. CONCLUSIONS	15
ACKNOWLEDGEMENTS	15
REFERENCES	16
APPENDIX A: MCC-1 TEST DATA AND NORMALIZED MASS LOSSES FOR BUFFER TESTS	49

FIGURES

	<u>Page</u>
1. Static Test Diagram	18
2. Single-Pass Flow-Through Test Diagram.....	18
3. Normalized Si Mass Losses from HIP Sodalite as a Function of Test Duration in Buffered Static Tests at 40°C.....	19
4. Normalized Si Mass Losses from HIP Binder Glass as a Function of Test Duration in Buffered Static Tests at 40°C.....	20
5. Normalized Si Mass Losses from HIP CWF as a Function of Test Duration in Buffered Static Tests at 40°C.....	22
6. Normalized Si Mass Losses from HIP Sodalite as a Function of Test Duration in Buffered Static Tests at 70°C.....	23
7. Normalized Si Mass Losses from HIP Binder Glass as a Function of Test Duration in Buffered Static Tests at 70°C.....	24
8. Normalized Si Mass Losses from HIP CWF as a Function of Test Duration in Buffered Static Tests at 70°C.....	25
9. Normalized Si Mass Losses from HIP Sodalite as a Function of Test Duration in Buffered Static Tests at 90°C.....	26
10. Normalized Si Mass Losses from HIP Binder Glass as a Function of Test Duration in Buffered Static Tests at 90°C.....	27
11. Normalized Si Mass Losses from HIP CWF as a Function of Test Duration in Buffered Static Tests at 90°C.....	28
12. Temperature and pH Dependencies of NR(Si) from Sodalite, HIP Binder Glass, and HIP CWF in Buffer Solutions.....	29
13. NL(Si) for Static Tests with HIP Sodalite, Glass, and CWF in Noncomplexing Buffer Solutions at 70°C vs. Test Duration.....	31
14. Normalized Si Mass Losses from Sodalite as a Function of Test Duration in Buffered Static Tests at 20°C.....	32
15. Normalized Si Mass Losses from HIP Glass as a Function of Test Duration in Buffered Static Tests at 20°C.....	33

FIGURES (continued)

	<u>Page</u>
16. Normalized Si Mass Losses from HIP CWF as a Function of Test Duration in Buffered Static Tests at 20°C.....	34
17. Dissolution Rate as a Function of Temperature and pH for Sodalite, HIP Glass, and HIP CWF	35
18. Normalized Si Mass Losses from PC Binder Glass as a Function of Test Duration in Buffered Static Tests at 70°C.....	37
19. Normalized Si Mass Losses from PC CWF as a Function of Test Duration in Buffered Static Tests at 20 and 70°C	38
20. Normalized Si Dissolution Rates as a Function of pH for PC Binder Glass at 70°C and PC CWF at 20 and 70°C	39
21. Normalized Si Mass Losses from Modified Glass as a Function of Test Duration in Buffered Static Tests at 70°C.....	39
22. Normalized Si Dissolution Rates as a Function of pH for Modified Glass and HIP Binder Glass as a Function of Test Duration in Buffered Static Tests at 70°C	40
23. Normalized Si Mass Losses as a Function of Test Duration from Static Tests on a Simple Five-Component Borosilicate Glass in Buffer Solutions at 70°C	41
24. Normalized Si Mass Losses as a Function of Test Duration from Static Tests on a CSG in Different S/V Ratios at 70°C	42
25. Results of SPFT Tests with CSG Glass at pH 9.5 and 70°C	43
26. NR(Si) vs. C ^{SS} (Si) for SPFT Tests at 70°C	44
27. NR(Si) vs. pH for Static and SPFT Tests at ANL and from KNAUSS [1990].....	45

TABLES

	<u>Page</u>
1. Chemical Composition of CSG and Modified Glasses	46
2. Compositions and Measured pH Values of Traditional Buffer Solutions at Test Temperatures	46
3. Properties of MES, PIPPS, and TEEN Buffers	46
4. Composition and Measured pH Values at 25, 40, and 70°C for Noncomplexing Buffers Used in Static Testing.....	47
5. Normalized Dissolution Rates of HIP Sodalite, Binder Glass, and Ceramic Waste Form as a Function of pH at 40, 70, and 90°C in Traditional and Noncomplexing Buffers.....	47
6. Regression Parameters for the Acid and Base Legs Corresponding to Equation 8	48
7. Model Parameters for Acid and Base Legs.....	48
A.1. Results of Static Tests on HIP Sodalite in Buffer Solution at 40°C	49
A.2. Results of Static Tests on HIP Binder Glass in Buffer Solution at 40°C.....	50
A.3. Results of Static Tests on HIP CWF in Buffer Solution at 40°C.....	51
A.4. Results of Static Tests on HIP Sodalite in Buffer Solution at 70°C	52
A.5. Results of Static Tests on HIP Binder Glass in Buffer Solution at 70°C.....	53
A.6. Results of Static Tests on HIP CWF in Buffer Solution at 70°C.....	54
A.7. Results of Static Tests on HIP Sodalite in Buffer Solution at 90°C	55
A.8. Results of Static Tests on HIP Binder Glass in Buffer Solution at 90°C.....	56
A.9. Results of Static Tests on HIP CWF in Buffer Solution at 90°C.....	57
A.10. Results of Static Tests on Sodalite in Noncomplexing Buffer Solution at 70°C.....	58
A.11. Results of Static Tests on HIP Binder Glass in Noncomplexing Buffer Solution at 70°C.....	59
A.12. Results of Static Tests on HIP CWF in Noncomplexing Buffer Solution at 70°C.....	59

TABLES (continued)

	<u>Page</u>
A.13. Results of Static Tests on Sodalite in Buffer Solution at 20°C.....	60
A.14. Results of Static Tests on HIP Binder Glass in Buffer Solution at 20°C.....	61
A.15. Results of Static Tests on HIP CWF in Buffer Solution at 20°C.....	62
A.16. Results of Static Tests on PC Binder Glass in Buffer Solution at 70°C	63
A.17. Results of Static Tests on PC CWF in Buffer Solution at 70°C	63
A.18. Results of Static Tests on Modified Glass in Buffer Solution at 70°C	64
A.19. Results of Static Tests on CSG Glass in Buffer Solution at 70°C	64
A.20. Results of Static Tests on CSG Glass with Three S/V Ratios at pH 9.4 Buffer Solution and 70°C	65
A.21. Results of SPFT Tests in pH 6.2 Buffer at Different Nominal F/S°	66
A.22. Results of SPFT Tests in pH 7.3 Buffer at Different Nominal F/S°	67
A.23. Results of SPFT Tests in pH 8.2 Buffer at Different Nominal F/S°	68
A.24. Results of SPFT Tests in pH 9.5 Buffer at Different Nominal F/S°	69
A.25. Steady-State Si Concentrations and Dissolution Rates	70

NOMENCLATURE

ANL	Argonne National Laboratory
ASTM	American Society for Testing and Materials
CSG	Component borosilicate glass
CWF	Ceramic waste form
EBR II	Experimental Breeder Reactor II
HIP	Hot isostatic pressing
ICP-AES	Inductively coupled plasma-atomic emission spectrometer
ICP-MS	Inductively coupled plasma-mass spectrometer
LLNL	Lawrence Livermore National Laboratory
NIST	National Institute of Standards and Technology
PC	Pressureless consolidation
SPFT	Single-pass flow-through tests
SRM	Standard Reference Materials
S/V	Surface area/volume of solution
TSPA	Total System Performance Assessment

**CORROSION TESTS TO DETERMINE TEMPERATURE AND pH
DEPENDENCIES OF THE DISSOLUTION RATES OF SODALITE, BINDER GLASS,
AND CERAMIC WASTE FORM**

Seung-Young Jeong, Thomas H. Fanning, Lester R. Morss, and William L. Ebert

ABSTRACT

A glass bonded-sodalite ceramic waste form (CWF) has been developed to immobilize salt wastes from electrometallurgical treatment of sodium-bonded spent nuclear fuel. The CWF is a composite of salt-loaded sodalite and a binder glass formed at high temperature (850-950°C) by hot isostatic pressing (HIP) or pressureless-consolidation (PC) processes. A waste form degradation and radionuclide release model has been developed to support qualification of the CWF for disposal in the proposed repository at Yucca Mountain. Six series of tests were conducted in conjunction with the development of that model. (1) Static tests were conducted to measure the dissolution rate of sodalite, HIP binder glass, and HIP CWF at 40, 70, and 90°C in pH range 4.8-9.8 buffer solution. The parameter values in the degradation model were calculated from the dissolution rates measured by the static tests. (2) Static tests were conducted at 70°C in noncomplexing tertiary amine pH buffers to confirm that the dissolution rate measured with traditional buffers was not affected by the complexation of metal ions. The results showed that the difference between dissolution rate determined with noncomplexing buffer and that determined with traditional buffers was negligible. (3) Static tests were conducted in five buffer solutions in the pH range 4.8-9.8 at 20°C with HIP sodalite, HIP glass, and HIP CWF. The results showed that the model adequately predicts the dissolution rate of these materials at 20°C. (4) Static tests at 20 and 70°C with CWF made by the PC process indicated that the model parameters extracted from the results of tests with HIP CWF could be applied to PC CWF. (5) The dissolution rates of a modified glass made with a composition corresponding to 80 wt% glass and 20 wt% sodalite were measured at 70°C to evaluate the sensitivity of the rate to the composition of binder glass in the CWF. The dissolution rates of the modified binder glass were indistinguishable from the rates of the binder glass. (6) The dissolution rate of a simple five-component glass (CSG) was measured at 70°C using static tests and single-pass flow-through (SPFT) tests. Rates were similar for the two methods; however, the measured rates are about 10X higher than the rates measured previously at Lawrence Livermore National Laboratory (LLNL) for a glass having the same composition using an SPFT test method. Differences are attributed to effects of the solution flow rate on the glass dissolution rate and how the specific surface area of crushed glass is estimated. This comparison indicates the need to standardize the SPFT test procedure.

1. INTRODUCTION

A glass-bonded sodalite ceramic waste form (CWF) degradation and radionuclide release model has been developed at Argonne National Laboratory (ANL) to predict CWF dissolution rates over long time periods and to support its qualification for disposal in a proposed nuclear waste repository at Yucca Mountain.

CWF has been developed to immobilize electrorefiner salt from electrometallurgical processing of spent sodium-bonded metallic nuclear fuel [PEREIRA-1997]. The CWF is composed of about 70 wt% salt-loaded sodalite, 25 wt% glass binder, and small amounts of halite and oxides. The CWF is prepared by first blending the zeolite 4A with waste electrorefiner salt at ~500°C to occlude the salt within cages of the zeolite crystal lattice. The salt-loaded zeolite is then mixed with a commercial borosilicate glass frit (75 wt% salt-loaded zeolite and 25 wt% glass) and heated to high temperature (850-915°C), at which temperature the salt-loaded zeolite transforms to sodalite, $\text{Na}_8(\text{AlSiO}_4)_6\text{Cl}_2$, and the melted glass encapsulates the sodalite. The CWF can be made using either a HIP process or a pressureless-consolidation (PC) process. The PC process has been selected for immobilizing electrochemically treated spent EBR II fuels.

A degradation model has been developed to support qualification of the CWF for disposal in the federal high-level waste disposal system. The dissolution behavior of the CWF is modeled by the expression

$$\text{rate} = k_0 \cdot 10^{(\eta \cdot \text{pH})} \cdot e^{(-E_a/RT)} \cdot (1-Q/K) + k_{\text{long}} \quad (1)$$

where

- rate = the dissolution rate of the CWF,
- k_0 = the intrinsic rate constant,
- η = the pH dependence,
- E_a = the activation energy,
- Q = the ion activity product of the solution,
- K = the apparent solubility product of the CWF, and
- k_{long} = the dissolution rate at saturation.

Values of the parameters k_0 , η , and E_a are determined under test conditions where the value of Q is maintained near zero, so that the value of the affinity term $(1-Q/K)$ remains near 1. The dissolution rate under conditions in which the value of the affinity term is near 1 is referred to as the forward rate. This is the highest dissolution rate that can occur at a particular pH and temperature. The value of the apparent solubility product, K, is determined from experiments in which the value of the ion activity product approaches the value of K. This results in a decrease in the value of the affinity term and the dissolution rate. k_{long} is included to account for the fact that dissolution of the binder glass does not cease when saturation ($Q/K=1$) is achieved. Since saturation is not achieved, k_{long} can be dropped from Equation 1.

The highly dilute solutions required to measure the forward rate and extract values for k_0 , η , and E_a can be maintained by conducting dynamic tests in which the test solution is removed from the reaction cell and replaced with fresh solution. In the single-pass flow-through (SPFT) test method, this is done by continuously pumping the test solution through the reaction cell.

Alternatively, static tests can be conducted with sufficient solution volume that the solution concentrations of dissolved glass components do not increase significantly during the test. Both the static and SPFT tests can be conducted over a wide range of pH values and temperatures. Both static and SPFT tests have shortcomings. The SPFT test requires analysis of several solutions (typically 6-10) at each of several flow rates to determine the glass dissolution rate at each pH and temperature. As will be shown, the rate measured in an SPFT test depends on the solution flow rate. In both the SPFT and static test methods, a compromise is required between the need to minimize the effects of dissolved components on the dissolution rate and the need to attain solution concentrations that are high enough to enable analysis. Although SPFT tests are commonly used to measure model parameter values, we used the static test to determine the model parameter values for hot isostatic pressing (HIP) of CWF. This is because the static test method has been standardized [ASTM-1998], whereas the SPFT test method has not been standardized, and far fewer tests and solution analyses are required to determine parameter values using the static test method than using the SPFT test method. In short-term static tests, the value of the affinity term $(1-Q/K)$ remains near one and the parameter values are readily determined from tests conducted at controlled temperature and pH. Tests in which the value of the affinity term is significantly lower than 1 can be identified by their deviation from a linear trend.

The tests described in this report were conducted to determine model parameter values and confirm the applicability of the model parameter values in the rate expressions for waste forms made by different process, with slightly different compositions, at temperatures outside the range used to determine the model parameters. The six series of tests are described below.

1. A series of static tests at 40, 70, and 90°C were conducted in traditional buffer solutions to determine the forward dissolution rates and to provide separate model parameter values (k_0 , η and E_a) for modeling the dissolution of sodalite, HIP binder glass, and HIP CWF. The forward dissolution rates, temperature, and pH dependence were used as components of a CWF degradation model to calculate the dissolution rate over long time periods in a nuclear waste repository.
2. Static tests with sodalite, HIP binder glass, and HIP CWF in noncomplexing tertiary amine pH buffers were carried out at 70°C to measure the forward dissolution rates at pH values between 5 and 9. These tests were done to confirm that the dissolution rates measured with traditional buffers were not affected by complexation of metal ions by the buffers.
3. A series of static tests was conducted in five dilute buffer solutions in the pH range of 4.8-9.8 at 20°C with sodalite, HIP binder glass and HIP CWF. The rates measured at 20°C were compared with the rate calculated with the CWF degradation model. These tests were conducted to confirm that the model adequately predicts the dissolution rates at lower temperatures.
4. Although model parameter values were determined during waste form development using materials made by HIP, a PC process has been developed and selected for the inventory reduction phase for EBR II waste. Tests and analyses have shown that the waste forms made by HIP and PC are almost identical. The major difference is that the PC CWF has a slightly higher porosity, and inclusion phases are more uniformly distributed throughout the binder glass in the PC CWF than in the HIP CWF. The dissolution rates of PC binder glass and PC CWF were measured in three buffer solutions in the pH range 6-9.5 at 70°C. These rates were

compared with the dissolution rates of HIP CWF under the same conditions to confirm that the model parameters determined from tests with HIP CWF could be applied to PC CWF.

5. The parameter values determined from tests with binder glass will be likely used to provide an upper bound to the dissolution rate of the CWF. Electron microscopy studies have shown that the size of sodalite inclusions decreases with process time, and the concentrations of silicon and aluminum in the binder glass near sodalite inclusions were higher than in binder glass further removed from the sodalite. These observations indicate that a small amount of the sodalite dissolves into the binder glass during processing. In order to evaluate whether changes in the binder glass composition due to the dissolution of small amounts of zeolite or sodalite affect the dissolution rates of the binder glass, we prepared a modified glass with a composition equivalent to a homogeneous mixture of 80 wt% glass and 20 wt% sodalite. A series of static tests with modified glasses were conducted in buffer solutions in the pH range 6.2-9.5 at 70°C to measure dissolution rates and compare with the rate measured with binder glass.
6. Static tests and SPFT tests in buffer solutions at 70°C were conducted with a simple five-component glass to demonstrate the validity of the static test method to measure the forward rate and model parameters. Static tests were conducted at low surface area to solution volume (S/V) ratios and for short durations to avoid solution feedback effects. The SPFT tests were conducted at several flow rates to determine the glass dissolution rate at each pH and temperature. The importance is that the results of SPFT tests with this glass were used to determine the temperature and pH dependence in the glass degradation model for Total System Performance Assessment (TSPA) [TRW-1998]. A flow-through apparatus at ANL has been constructed and used to repeat the measurements of dissolution rates with the simple five component glass at several pH values. It is expected that these tests will provide a link between the static tests used to measure model parameters for the CWF with the SPFT tests used to measure model parameters used in the TSPA glass model.

2. EXPERIMENTAL METHODS

2.1 STATIC TEST PROCEDURE

Static tests were conducted following the American Society for Testing and Materials standard test method C 1220 [ASTM-1998] in Teflon® containers with buffer solutions. Briefly, tests are conducted by immersing a monolithic sample with a known geometric surface area in a volume of fluid such that the S/V ratio is 10 m⁻¹. The test vessel is sealed and placed in a constant temperature oven for a prescribed duration. At the end of the test, the test solution is analyzed for dissolved components of the test specimen. To achieve an S/V ratio of 10 m⁻¹, a typical polished wafer with total surface area of 2.00 cm² was placed in a buffer solution of volume 20.00 mL. The Teflon vessels were placed in a secondary container that was partially filled with demineralized water to provide nearly equal water vapor pressures inside and outside the vessel to minimize loss of solution during the test. The secondary container was placed in a constant-temperature oven for the duration of the test. Figure 1 is a diagram of the static test.

Tests were conducted at 20 and 40°C for durations of 7, 14, 28, 56, and 91 days; at 70°C for durations of 2, 3, 5, 7, and 10 days; and 90°C for duration of 1, 2, 3, and 5 days. The tests at 20 and 40°C were run for longer durations to ensure that solution concentrations of matrix elements would be high enough to measure. Tests at shorter durations showed the effects of surface roughness and tests at longer durations showed the effect of the affinity term (1-Q/K).

Termination of the tests required taking aliquots for three analytical measurements. Two aliquots were taken to measure the pH of the test solution. The pH of the first aliquot was measured at the test temperature. The pH of the second aliquot was measured at room temperature. Mean pH values at each temperature were calculated from 3-5 measurements of pH. The pH measurements at test temperature were done immediately after termination by placing the vial in a water bath at the test temperature. The room temperature measurements were done several minutes later; the filled 1.5-mL solution vials were sealed until measurement to minimize CO₂ contamination. The remaining test solution, about 20 mL, was passed through a 0.45-μm pore-size filter, acidified and submitted for inductively coupled plasma-atomic emission spectrometer (ICP-AES) or inductively coupled plasma-mass spectrometer (ICP-MS) analysis.

The extent of dissolution for each test duration was calculated as the normalized mass loss by dividing the concentration of silicon in solution by the S/V ratio used in the test and by the mass fraction of Si in the glass:

$$NL(Si) = C(Si) / [(S/V) \cdot f(Si)] \quad (2)$$

where

NL(Si) = normalized mass loss of element Si, g/m²,
 C(Si) = concentration of element Si in the test solution, mg/L,
 S = surface area of material in the test, m²,
 V = volume of solution in the test, m³, and
 f(Si) = mass fraction of element Si in the material.

The normalized dissolution rate, NR (Si), g/(m²d), was determined as the slope of a plot of NL(Si) versus the test duration, t, as

$$NR(Si) = \Delta NL(Si) / \Delta t \quad (3)$$

Individual regression fits for each material, temperature, and pH were plotted to determine the dissolution rate. The dissolution rates were used to calculate the parameters for modeling. The solution was presumed not to affect the dissolution rate as long as NR(Si) was constant. A decrease in the value of NR(Si) as the test duration increases indicates that the buildup of silicon in solution is slowing the glass dissolution. Tests in which the rate has clearly been affected by solution feedback effects were excluded from the regression.

2.2 SINGLE-PASS FLOW-THROUGH TESTS

The SPFT tests were conducted by continuously pumping a solution through a reaction cell that contained the glass and collecting the effluent for analysis. The glass dissolution rate was

calculated from the steady-state solution concentration of Si and solution flow rate by using the expression

$$NR(Si) = [C^{ss}(Si) \cdot (F/S^\circ)] / f(Si) \quad (4)$$

where

NR(Si) = normalized dissolution rate, g/(m²d),

C^{ss}(Si) = steady-state concentration of Si in effluent, mg/L,

F = solution flow rate, mL/s,

S[°] = initial surface area of the crushed glass, m², and

f(Si) = mass fraction of Si in the glass.

In SPFT tests, different steady-state concentrations are attained at different solution flow rates. This results in different values of the affinity term and different glass dissolution rates occurring at different flow rates. The dependence of the rate measured in SPFT tests on the solution flow rate must be taken into account to determine the forward rate. We conducted the tests at several flow rates to measure the rate at several steady-state concentrations of Si, then plotted the rate against the steady-state concentration and extrapolated to zero concentration. The y-intercept was taken to be the forward dissolution rate.

The SPFT tests were conducted with crushed glass to provide a high surface area. The CSG glass was crushed and sieved to isolate the -40 +60 mesh (425 μm to 250 μm) size fraction. The crushed glass was washed repeatedly with absolute ethanol to remove fines. Some of the glass was examined with a scanning electron microscope to verify all fines had been removed and the particles were the expected size. The specific surface area of the crushed glass was calculated to be 0.0071 m²/g by assuming the particles were spheres having a diameter equal to 338 μm, which is the arithmetic average of the sieve sizes. This is the method recommended for static tests conducted with crushed glass [ASTM-1999].

The SPFT apparatus was constructed using a variable speed peristaltic pump and polyethylene tubing. Various pump speeds and tubing diameters were used to achieve a range of flow rates, and different amounts of glass were used to vary the surface area and achieve a range of F/S[°] values. A modified polyethylene pipette tip was used as a reaction cell. Polyethylene wool was used to prevent sample from being flushed from the cell during the test. Tests were conducted with between 1 and 3 g of glass. The glass was not constrained within the reaction cell, and the solution flowed upward through the glass. The reaction cell and was housed in a constant-temperature oven set at 70°C. Approximately 1 m of tubing was placed in the oven ahead of the reaction cell to heat the solution to 70°C. The tubing exiting the reaction cell was kept as short as possible so that the effluent solution could be collected soon after it left the reaction cell to minimize the time lag. Figure 2 is a diagram of the SPFT test apparatus designed at ANL.

Effluent solution was collected periodically in polyethylene solution bottles for analysis. The mass of each sample aliquot and the time it was collected were used to calculate the flow rate. The solutions were analyzed with an ICP-MS. All solutions collected at a particular pH, temperature, and flow rate were analyzed in the same group to eliminate effects of the day-to-day variability of the ICP-MS. Control tests were conducted without glass to verify that interactions between the buffers and the apparatus were negligible.

2.3 SAMPLE PREPARATION

Monoliths of salt-loaded sodalite were prepared from granular zeolite 4A containing up to 10% clay binder that had been blended with simulated electrorefiner salt at 500°C and heated to 850-915°C in HIP. The binder glass and CWF were prepared by HIP processing and by PC processing. The HIP CWF was prepared by first blending the zeolite 4A with waste electrorefiner salt at ~500°C to occlude the salt within cages of the zeolite crystal lattice. The salt-loaded zeolite is mixed with a commercial borosilicate glass frit (75 wt% salt-loaded zeolite and 25 wt% glass) and heated under pressure at high temperature (850-915°C), at which the salt-loaded zeolite transforms to sodalite, $\text{Na}_8(\text{AlSiO}_4)_6\text{Cl}_2$, and the melted glass encapsulates the sodalite. The PC binder glass was prepared from commercial borosilicate glass heated at 915°C for 16 hours; the PC CWF was prepared from the commercial binder glass and zeolite 4A loaded with simulated 300-driver salt heated under the same conditions. The CWF is composed of about 70 wt% salt-loaded sodalite, 25 wt% binder glass, and small amounts of halite and oxides.

Modified glass was batched from oxides and carbonates to yield a composition equivalent to a homogeneous mixture of 80 wt% glass and 20 wt% sodalite. This composition represents a likely upper bound for the amount of zeolite and sodalite that may dissolve into the binder glass during processing. The oxide and carbonate reagents were mixed, heated in Pt/Rh crucibles to 500°C to decompose carbonates, then heated to 1150°C and held at this temperature for one hour. The mixture was quenched to room temperature, but it was noted that the glass was not homogeneous. The material was crushed to -60 mesh, remelted at 1500°C, poured into a mold, cooled at a rate of 24°C/hour to 550°C, annealed for two hours at 550°C, and furnace-cooled to room temperature. This resulted in a homogeneous glass.

A simple five-component borosilicate glass (CSG) was batched from oxides and carbonates to yield a composition identical to that described by Knauss et al. [KNAUSS-1990]. The oxide and carbonate reagents were mixed, heated in Pt/Rh crucibles to 500°C, held at 500°C for 30 min, heated to 800°C and held overnight to decompose carbonates, heated to 1150°C and held at this temperature for one hour, quenched to room temperature, and crushed to -60 mesh. The crushed glass was remelted at 1150°C, poured into a mold, cooled at a rate of 24°C/hour to 550°C, annealed for two hours at 550°C, and furnace-cooled to room temperature. This resulted in a homogeneous glass.

Samples of CSG and modified glasses were crushed to -100 +200 mesh to yield 0.5 g of each glass for chemical analysis. These samples were dissolved and analyzed by standard procedures. The compositions are shown in Table 1.

Cores were drilled with a drill press and a diamond-coring bit using absolute ethanol as coolant. The circumferences (edges) of the cores were polished to 600 grit on a jig (attached to the Buehler low-speed saw) that rotates the cores. The cores were cut into wafers on a Buehler Isomet low-speed saw with diamond wafering blades using absolute ethanol as coolant/lubricant. The faces of the wafers were polished to 600 grit on a Metaserv 2000 grinder/polisher. After polishing, all wafers were examined using an optical microscope to ensure that the surface finishes were uniform. The dimensions of the polished wafers were measured using precision calipers. The pellets were washed once with absolute ethanol in an ultrasonic bath. Water or ethanol-water mixtures washes were not performed to avoid dissolving halite exposed at the surface. The pellets were dried in a 40°C oven overnight and stored in a desiccator.

2.4 BUFFER SOLUTION PREPARATION AND PH MEASUREMENT

Buffer solutions having the compositions and pH values in Table 2 were prepared for use in static tests. The buffer solutions were selected to minimize chemical interactions with components of glass and sodalite. Concentrations were selected to maintain nearly constant ionic strength and adequate buffering capacities to maintain pH within 0.1 pH unit.

The pH was determined using an Orion Ross “spear-tipped” combination semi-micro electrode attached to a Fisher Accumet Research AR 50 meter. The combination electrode was calibrated using buffer solutions maintained at the test temperatures with a constant-temperature bath. Disposable 1.5-mL centrifuge tubes that had a profile similar to that of the spear-tipped electrode were used so that the amount of buffer solution or test solution necessary for measurement was minimized. The centrifuge tubes were held in a punched aluminum tray on the surface of the bath.

The combination electrode was calibrated prior to use with standard commercial buffers (Ricca Chemicals). These buffers are pH 4.00, 7.00 and 10.00 at 25°C, and have NIST-traceable pH values for temperatures 50°C. The 70°C and 90°C pH values were determined by extrapolation. The calibration and extrapolation were confirmed with pH values provided by Bates [BATES-1973]. The buffer composition and pH values are as shown in Table 2 for several temperatures.

Standard Reference Materials (SRM) from the National Institute of Standards and Technology (NIST) were used to make buffer solutions to calibrate the pH electrode at temperatures above 50.0°C. The NIST certificates [NIST-1991, -1996, -1998] tabulate the certified pH values up to 50.0°C. For pH values at higher temperatures, NIST [1991] was used. It is also advantageous to use NIST standards because they are more accurate than standards made by secondary manufacturers. The NIST standard buffer solutions were prepared from NIST SRM potassium dihydrogen phosphate (SRM 186-I-f), disodium hydrogen phosphate (SRM 186-II-f), Na₂B₄O₇•10H₂O (borax, SRM 187d), and potassium hydrogen phthalate (SRM 185g).

Three noncomplexing buffers (MES, PIPPS, and TEEN) were selected from a set of "better" buffers proposed by Rorabacher and Kandedgedara [RORABACHER-1999]. The properties of MES, PIPPS, and TEEN are given in Table 3.

These buffering systems have been shown to not to complex significantly with metal ions. The new noncomplexing tertiary amine buffer compounds used for the pH buffered static test modification were: (1) 2-(N-morpholino)ethanesulfonic acid (MES), (2) piperazine-N,N'-bis(3-propanesulfonic acid) (PIPPS), and (3) N,N,N,N'-tetraethylethylenediamine (TEEN).

In preliminary tests, it was established that there is significant decomposition of TEEN within one day (pH change of 0.5 pH units or more) at 90°C, but no significant decomposition of MES, PIPPS, or TEEN at 70°C over one week (pH change of 0.01 M buffers of less than 0.2 pH units). Buffer solutions of MES, PIPPS, and TEEN and measured pH values at 25, 40, 70°C are listed in Table 4.

3. CALCULATION OF TEMPERATURE AND pH DEPENDENCIES

3.1 STATIC TESTS IN TRADITIONAL BUFFER SOLUTIONS AT 40, 70, AND 90°C

A series of static tests in traditional buffer solutions (Table 2) at 40, 70, and 90°C were conducted to measure forward dissolution rates for sodalite, HIP binder glass, and HIP CWF and to provide model parameter values (k_0 , η , and E_a). The forward dissolution rates, temperature, and pH dependence were used as components of a CWF degradation model.

The concentration of Si in solution provides the best measure of matrix dissolution of glass-bonded sodalite, since Si is a main structure element in both the glass and sodalite. The measured Si concentrations in solutions from buffered static tests with each material (sodalite, binder glass, and CWF) were used to calculate the normalized mass loss of Si [NL(Si)], defined as Equation 2. At each temperature and pH, the concentration of Si increased rapidly during the shortest test durations, then increased at a slower but nearly linear rate for long test durations. The Si concentrations and normalized mass losses are listed in Tables A.1-A.9 of Appendix A for each material, temperature, and pH.

Normalized dissolution rates, NR(Si), were calculated by linear regression. Individual regression fits for each material, temperature, and pH are shown in Figures 3 through 11. The results of the regression fits are summarized in the boxes in each of the figures. The linear fit is expressed as

$$y = m_1 + m_2 \cdot MO \quad (5)$$

where m_1 is the y-intercept and m_2 is the slope; MO is the test duration. The goodness of fit is given as chi squared (Chisq) and as the regression coefficient R. The slope gives the forward dissolution rate. Some test results (outliers) were excluded from the regression fits; these are shown as open symbols in the plots. The dissolution rates determined from the slope of each regression fit are summarized in Table 5. Dissolution rates as a function of pH are plotted at 40, 70, and 90°C for each material with closed symbols in Figure 12.

3.2 STATIC TESTS IN NONCOMPLEXING BUFFER SOLUTIONS

Static tests with sodalite, HIP binder glass, and HIP CWF in noncomplexing tertiary amine pH buffers were carried out at 70°C to confirm that the dissolution rates measured with traditional buffers were not affected by complexation. The test results using noncomplexing pH buffer were compared with the dissolution rates using traditional buffers. Figure 13 shows the values of NL(Si) from sodalite, HIP binder glass, and HIP CWF in noncomplexing buffer solutions at 70°C as function of test duration. Experimental data and NL(Si) results are compiled in Tables A.10, A.11, and A.12 in Appendix A. Normalized dissolution rates were determined from the slopes of each linear regression fit for tests with sodalite, HIP glass, and HIP CWF at temperature 70°C with noncomplexing buffer solutions. These dissolution rates are included in Table 5. The dissolution rates measured with the noncomplexing buffer solutions as function of pH are included in Figure 13. The results show that the difference between dissolution rates measured with noncomplexing buffers and with traditional buffers is negligible. Figures 12a and 12c show that the dissolution behaviors of sodalite and the CWF are similar with both traditional and noncomplexing buffers.

3.3 MODEL PARAMETER VALUES

The dissolution behavior of the CWF is modeled by Equation 1. Long-term PCTs are conducted to obtain values for K and k_{long} and to provide insight into the material behavior at advanced stages of corrosion. The parameters K and k_{long} are usually obtained from PCTs with duration longer than one year. As described above, short-term MCC-1 tests were used to determine the forward rate. In MCC-1 tests conducted at low surface-to-volume ratios and short test durations, the orthosilicic acid activity remains low and the value $(1-Q/K)$ remains near one. Since the test solutions are maintained far from saturation, k_{long} can be dropped from Equation 1. This leaves

$$\text{rate} \approx k_f = k_o \cdot 10^{(\eta \cdot \text{pH})} \cdot e^{(-E_a/RT)} \quad (6)$$

When the logarithm of Equation 6 is taken, a linear expression is obtained:

$$\log(k_f) = \log k_o + \eta \cdot \text{pH} - \{E_a/(R \ln 10)\} \cdot T^{-1} \quad (7)$$

The values of η and E_a can be obtained by performing a linear regression on the logarithm of the normalized dissolution rates as a function of pH and temperature, respectively. Linear regression of the dissolution rates in Table 5 was performed using separate regression fits for the rates measured acidic and alkaline buffers.

The pH and temperature dependence on the dissolution rates for each material was fit to the function

$$\log k_f = C_0 + C_1(\text{pH} - C_{\text{pH}}) + C_2(1/T - C_T) \quad (8)$$

where C_0 , C_1 , and C_2 represent regression coefficients. The constant C_{pH} and C_T represent the average pH and average inverse temperature, respectively, of the data used in the regression. The resulting coefficients and standard errors for each fit are shown in Table 6. Equation 8 is plotted in Figure 12. for each material at 40, 70, and 90°C. The dissolution rate parameters k_o , η , and E_a can be determined by comparing Equation 8 with Equation 7 to show that $\log k_o = C_0 - C_1 C_{\text{pH}} - C_2 C_T$; $\eta = C_1$; and $E_a = C_2 R \ln 10$. These parameters are shown in Table 7.

The dissolution rates measured for CWF reflect the simultaneous dissolution of sodalite and binder glass phases. A comparison of Figures 12a and 12c shows similar dissolution behavior between sodalite and the CWF. This is due to the forward dissolution rate of sodalite being higher than that of the glass, and to the fact that sodalite composes approximately 70 wt% of the CWF. Sodalite dissolves faster than binder glass under these test conditions over much of the pH range tested. However, because of the weak pH dependence of sodalite dissolution, glass is predicted to dissolve faster than sodalite above pH 9.

We point out that these tests were designed to measure the forward dissolution rate and the effects of pH and temperature in the absence of solution feedback effects, i.e., when the values of the affinity term is one. Under actual disposal conditions, the affinity term will have a significant effect on the CWF dissolution rate.

In the Yucca Mountain disposal system, the incoming groundwater can be assumed to be in equilibrium with cristobalite (a major constituent of the host rock at Yucca Mountain), and the value of Q in Equation 1 will be set by the solubility of cristobalite. The solubility of sodalite is much lower than that of cristobalite, suggesting that the affinity term $(1-Q/K)$ in Equation 1 will tend toward zero for the sodalite phase of the CWF. The binder glass is much more soluble than cristobalite because the binder glass is predicted to dissolve faster than sodalite in tuff groundwater under repository conditions. The model parameter values measured for the binder glass are used to model the CWF dissolution rate in repository calculations.

3.4 PREDICTABILITY OF RATE EXPRESSION

A series of static tests were conducted using five buffer solutions in the pH range of 4.8-10 at 20°C with sodalite, HIP binder glass, and HIP CWF. These tests were conducted to confirm that the model parameters derived from tests at 40, 70, 90 °C could be used to predict the dissolution rates at a lower temperature.

Values of $NL(Si)$ for tests with sodalite, HIP binder glass, and HIP CWF as functions of test duration are shown in Figures 14-16. Normalized dissolution rates $[NR(Si)]$ were obtained by linear regression of the $NL(Si)$. The $NL(Si)$ results were used in the linear regressions except for obvious outliers. Outliers are shown as open circles in Figures 14-16.

For each material, the $NR(Si)$ values are plotted as a function of pH in Figure 17. As was the case for the forward dissolution rate at 40, 70, and 90°C, the $NR(Si)$ from sodalite, HIP binder glass, and HIP CWF at 20°C have negative slopes in acidic solutions and positive slopes in basic solutions, with minima near neutral pH. The V-shaped lines in Figure 17 were obtained from the regression fits for the dissolution rates of the HIP sodalite, binder glass, and CWF in acid and basic regions from 40, 70, 90°C test results. The lowest V-shaped lines in Figure 17, representing 20°C dissolution rates, were calculated from the rate expression in Equation 6 using the regression fits derived from tests at higher temperatures. The reason for this deviation is not known.

The Si concentrations in several of the test solutions, in particular those from the binder glass, were very low (near the ICP-MS detection limits). Analytical uncertainties and possible contaminants from previously used test vessels or leakage from 20°C water bath increase the scatter of the 20°C test results. Nevertheless, the deviations of the $NR(Si)$ from the V-shaped model prediction lines in Figure 17 were small. We note that the $NR(Si)$ points at pH 4.8 of sodalite and CWF are significantly higher than model prediction lines.

These results indicate that the model parameters measured for HIP CWF over the temperature range of 40-90°C can be used to adequately predict the dissolution rate at 20°C.

3.5 EFFECT OF CWF CONSOLIDATION METHOD

Static tests were conducted with PC binder glass and PC CWF in three buffer solutions in the pH range 6-10 at 20 and 70°C to confirm that the parameter values determined from materials made by HIP (i.e., the values in Table 6) could be applied to materials made by PC. The PC binder glass was prepared from commercial borosilicate glass heated at 915°C for 16 hours; the PC CWF was prepared from the commercial binder glass and zeolite 4A loaded with simulated 300-driver salt heated under the same conditions. Static tests were conducted using buffer solutions at pH 6.2, 8.2,

and 9.5 at 70°C with PC binder glass and CWF, and at pH 5.95, 8.37, and 9.81 at 20°C with PC CWF. Composition and measured pH values at 20 and 70°C for buffers used in the static test are listed in Table 3.

The normalized Si mass losses from PC binder glass and PC CWF as functions of test duration are shown in Figures 18 and 19. The normalized Si dissolution rates were obtained by linear regression of the normalized Si mass losses. For each PC material, the dissolution rate values are plotted as a function of pH and compared with dissolution rates of HIP material in Figure 10. The NR(Si) from binder glass and CWF prepared under HIP or PC conditions have negative slopes in acidic solutions and positive slopes in basic solutions, with minima near neutral pH. The V-shaped lines in Figure 20 were obtained by using separate regression fits for the dissolution rates of the HIP binder glass and CWF in acid and basic regions. The pH dependence for the forward dissolution rates of PC binder glass and CWF were indistinguishable from those of HIP binder glass and CWF at 20 and 70°C within the test uncertainty. These results show that the model parameters determined from the results of tests with HIP CWF can be applied to PC CWF.

3.6 EFFECT OF GLASS COMPOSITION

Electron microscopy studies of sodalite granules and the intergranular binder glass in HIP CWF showed that the concentrations of silicon and aluminum in the binder glass within ~20 micrometers of the glass-sodalite phase boundaries were greater than those in the unprocessed binder glass. This may indicate that small amounts of zeolite or sodalite dissolved into the binder glass during the consolidation. In order to evaluate whether changes in the binder glass composition due to the dissolution of small amounts of zeolite or sodalite during processing affect the dissolution rates of the binder glass, we prepared a modified binder glass to represent glass with dissolved sodalite. Its dissolution rate was measured as a function of pH with buffered static tests at 70°C. The preparation of the modified glass is described in Section 2.

The static tests in the three noncomplexing buffer solutions were conducted to determine the dissolution rates of the modified glass at 70°C as a function of pH. The buffer solutions at 70°C had pH values of 6.2, 8.2, and 9.5; the buffer compositions are listed in Table 2. The NL(Si) from tests with the modified glass as function of test duration are shown in Figure 21. The NR(Si) were obtained by linear regression of the normalized Si mass losses as shown in Figure 22. In Figure 22, the dissolution rates of the modified glasses were compared with the dissolution rates of HIP binder glass. The V-shaped line in Figure 22 is from the model parameters derived from the dissolution rates of the HIP binder glass at 40, 70, and 90°C. The NR(Si) for the modified glass and its pH dependence in the basic region were consistent with those of the binder glass at 70°C. These results indicate that the dissolution rate of the glass in CWF adjacent to sodalite domains is the same as the dissolution rate of the unaltered binder glass.

3.7 STATIC TESTS AND SINGLE-PASS FLOW-THROUGH TEST WITH CSG GLASS

3.7.1 Static Test Method

Static tests in buffer solutions at 70°C were conducted with a simple five-component (Al, B, Ca, Na, Si) borosilicate glass (CSG) to demonstrate the validity of the static method to measure the forward rate. The results of static tests will be compared with the forward dissolution rates measured with flow-through tests previously at LLNL [KNAUSS-1990] and recently at ANL (see

Section 3.7.2). The importance of comparing static and SPFT tests is that the results of flow-through tests by LLNL were used to determine the temperature and pH dependencies in the glass degradation model for Total System Performance Assessment calculation for Site Characterization of the Yucca Mountain disposal system [TRW-1998], whereas static test are used to measure these dependencies for CWF.

Figure 23 shows the results of static tests conducted with CSG glass at 70°C in buffer solutions at pH 6.2, 7.3, 8.2, and 9.5. Each point represents the results of a separate test, and the uncertainty bars are drawn at 15% of the measured value to account for analytical uncertainty. The regression lines drawn through the data give the dissolution rates at the three pH values. As discussed in following sections of this report, we suspect that dissolution in the pH 9.5 tests beyond about 5 days is slowed by the buildup of silicon in the solution, and those results were excluded from the regression fit. The static tests were conducted with pH 9.4 buffer solution using shorter durations (1- to 5-day) and lower S/V ratios (10, 5, and 2.5 m⁻¹) to measure forward rate without feedback effects, as shown in Figure 24. As a result, the value of the affinity term decreases as S/V increases. A dissolution rate of 0.72 g/(m²•d) was measured in tests at S/V=10 m⁻¹ and a rate of 1.33 g/(m²•d) was measured in tests at S/V=2.5 m⁻¹ (see Appendix A, Table A.20). The regression lines in Figures 23 and 24 all have positive y-intercepts. This is probably a result of the slight surface roughness.

3.7.2 Single-Pass Flow-Through Tests

Figure 25a shows silicon concentrations in the aliquots from SPFT tests conducted at pH 9.5 and different F/S° values. The set of data at each F/S° represents the aliquots of effluent solution collected sequentially during the test. The average flow rate for each set of aliquots in a test was used to calculate the value of F/S° for that test. The steady-state Si concentration for each test was determined as the average of the last five aliquots. The values of F/S°, Si concentration and dissolution rate for pH 6.2, 7.3, 8.2, and 9.5 are listed in Table 3 A.21-23 in Appendix A. The steady-state Si concentration and the values of F/S° for pH 6.2, 7.3, 8.2 and 9.5 are listed in Table A.24 in Appendix A. Higher concentrations were sometimes measured in the first several samples due to the dissolution of high-energy sites (e.g., sharp ends of glass shards). The dissolution rate for each test was calculated using Equation 4. For example, the steady-state Si concentration for the test conducted at pH 9.5 and F/S° = 3.98 x 10⁻⁷ m/s was C^{ss}(Si) = 8.2 mg/L and the mass fraction of Si in the CSG glass is f(Si) = 0.277. The dissolution rate is 1.04 g/m².

Figure 25b shows the measured rate plotted against the value of F/S°. The rate initially increases with the value of F/S° and then levels off at an F/S° value of about 1 x 10⁻⁶ m/s. This is in response to the value of the affinity term increasing to about 1 as F/S° increases. The point at which the rate becomes constant corresponds to the affinity term becoming 1 and the glass dissolving at its forward rate. Comparison of Figures 25a and 25b indicates that Si concentrations greater than about 8 mg/L are sufficient to slow the glass dissolution rate at 70°C and pH 9.5. This observation is used later in the analysis of static tests.

Because of scatter in the data and experimental uncertainty, it is difficult to determine the forward rate from the plot in Figure 25b. Instead, we have plotted the rates against the steady-state silicon concentrations in Figure 26. The measured rates are linearly regressed and the y-intercept (at a silicon concentration of 0) gives the forward rate. The scatter in the experimental results at low silicon concentrations has only a minor impact on determining the rate.

3.7.3 Discussion

The dissolution rates measured at ANL using static leach tests ($S/V = 2.5 \text{ m}^{-1}$ at pH 9.4 and $S/V = 10 \text{ m}^{-1}$ at pH 6.2, 7.3, and 8.2) and SPFT tests are compared with SPFT results of LLNL in Figure 27. The rates measured using static test and SPFT test at ANL are the same at pH 6.2, 7.3, and pH 9.4, but differ slightly at pH 8.2. As noted earlier, Si concentrations $>8 \text{ mg/L}$ appeared to affect the dissolution rate in the SPFT tests. In the static tests, a Si concentration of 8 mg/L would result in a $NL(\text{Si})$ value of about 3 g/m^2 . Static tests at pH 9.5 and $S/V = 10 \text{ m}^{-1}$ conducted for 10 days resulted in Si concentrations that were $>8 \text{ mg/L}$ and $NL(\text{Si})$ that were $>3 \text{ g/m}^2$. In the extreme case of fitting the line through only the 2- and 3-day results at pH 9.5, the rate is about $0.90 \text{ g/(m}^2 \cdot \text{d)}$, which is still significantly lower than the rate of $1.7 \text{ g/(m}^2 \cdot \text{d)}$ measured with the ANL SPFT tests. The Si concentration measured in the 5-day test at pH 9.4 in tests conducted at $S/V = 2.5 \text{ m}^{-1}$ was 4.7 mg/L . Its dissolution rate was $1.3 \text{ g/(m}^2 \cdot \text{d)}$, which is similar to the ANL SPFT result. This suggests that the results of static tests conducted for 7 and 10 days with $S/V = 10 \text{ m}^{-1}$ at pH 9.5 and 70°C should not be used to determine the forward rate. The concentrations in all tests at pH 8.2, 7.3, and 6.2 are $<8 \text{ mg/L}$.

The results of SPFT tests with CSG glass conducted by Knauss et al. are included in Figure 27. Their measured rates are significantly lower than what we measured with either the static or SPFT test methods. Differences in the SPFT test results may be due to differences in how the tests were conducted and how the data were analyzed. Crushed glass of the $-100 +200$ mesh size fraction was used in SPFT tests conducted by Knauss et al. and by us. Knauss et al. measured the surface area of crushed CSG glass to be $485 \text{ cm}^2/\text{g}$ by gas adsorption and used that value to calculate the dissolution rate. For comparison, the geometric surface area calculated from the average particle size (which was $100 \text{ }\mu\text{m}$) is $234 \text{ cm}^2/\text{g}$. From Equation 4, the calculated rate is inversely proportional to the surface area. The rates measured by Knauss et al. would be about 2X higher if they were calculated using the geometric surface area rather than the gas adsorption surface area. Nevertheless, the rates of Knauss et al. would still be about 10X lower than the values we measured.

Additional experimental details regarding the test method used by Knauss et al. were provided in a subsequent paper [KNAUSS-1990]. Those conditions were compared with our results to evaluate possible contributions of test conditions to the difference in the results. The SPFT tests of Knauss et al. were run with about 1 g of glass and at flow rates up to 60 mL/day. Using the geometric surface area of $234 \text{ cm}^2/\text{g}$, the typical F/S° value for those tests is about $3 \times 10^{-8} \text{ m/s}$. At pH 10, the steady-state Si concentration was about 13 mg/L (from Table 9 in reference [BATES-1992]). Our tests at pH 9.5 and $F/S^\circ = 3.0 \times 10^{-8} \text{ m/s}$ gave a steady-state Si concentration of about 24 mg/L (see Figure 25a). The results in Figure 25b indicate that Si concentrations greater than about 8 mg/L are expected to decrease the glass dissolution rate. This suggests that the dissolution rates measured by Knauss et al. were slowed by feedback effects. However, it is stated in [KNAUSS-1990] that doubling the flow rate after steady state was reached did not measurably affect the dissolution rate. It is uncertain how much of the differences in SPFT test results are due to experimental design, test execution, and data interpretation.

The American Society for Testing and Materials (ASTM) Nuclear Fuel Cycle subcommittee C26.13 is working to standardize the SPFT test method so that results obtained in different laboratories can be compared directly. The SPFT tests discussed in this report were conducted, in part, to help develop a standard test procedure, identify the test conditions that need to be tracked and reported, and develop a standard method for data analysis and determination of the dissolution

rate. An inter-laboratory study will be conducted in the near future to measure the precision of SPFT tests.

4. CONCLUSIONS

Tests were conducted with glass-bonded ceramic waste form (CWF) and its major constituents, binder glass and sodalite, to provide parameter values for the degradation and radionuclides release model that has been developed for evaluating the impact of the CWF on the performance of the proposed repository at Yucca Mountain. Static tests in traditional buffer solutions at 40, 70, and 90°C were conducted to determine model parameter values for dissolution of sodalite, HIP binder glass, and HIP CWF.

The results of our tests have led to the following findings:

- Within experimental uncertainty, the differences between dissolution rates determined with noncomplexing buffers and those with traditional buffers are negligible. Therefore, we confirmed that the forward rates determined at 40, 70, and 90°C from static tests with traditional buffers are valid. Model parameter values were calculated using the dissolution rates measured with traditional and noncomplexing buffers.
- The CWF degradation model using parameters measured for HIP CWF over the temperature range of 40-90°C can adequately predict the dissolution rate at 20°C. This was shown by the results of a series of static tests in five buffer solutions in the pH range of 4.8-9.8 at 20°C with sodalite, HIP glass, and HIP CWF.
- The CWF degradation model using parameters measured for HIP CWF can also be applied to PC CWF. The pH and temperature dependences for PC glass and PC CWF are similar to those for HIP glass and HIP CWF.
- The rate expression for dissolution of the binder glass is not sensitive to small or moderate changes in the glass composition. The dissolution rates of a glass with a composition corresponding to 80% binder glass and 20% sodalite were consistent with the dissolution rates of the binder glass at 70°C.
- The same dissolution rate of a simple five-component borosilicate glass (CSG) was measured with the static and single-pass flow-through (SPFT) tests. The measured rates are about 10X higher than the rates measured previously for a glass having the same composition using SPFT tests at LLNL. Differences are attributed to effects of the solution flow rate on the glass dissolution rate and how the specific surface area of crushed glass is estimated. This comparison indicates the need to standardize the SPFT test procedure.

ACKNOWLEDGEMENTS

The authors acknowledge the scientific collaboration and advice of M. A. Lewis, Y. Tsai, and S. F. Wolf. This work was supported by the U. S. Department of Energy, Office of Nuclear Energy, Science and Technology, under contract W-31-109-ENG-38.

REFERENCES

[ASTM-1998]

American Society for Testing and Materials, *Annual Book of ASTM Standards*, **12.01**, "Standard Test Method for Static Leaching of Monolithic Waste Forms for Disposal of Radioactive Waste," C1220-98, 1-16 (1998).

[ASTM-1999]

American Society for Testing and Materials, *Standard Test Methods for Determining the Chemical Duration of Nuclear Waste Glasses: The Product Consistency Test (PCT)*, American Society for Testing and Materials standard C1285-97, Annual Book of ASTM Standards, West Conshohocken, Pennsylvania (1999).

[BATES-1973]

Bates, Roger Gordon, *Determination of pH*. John Wiley & Sons, New York (1973).

[BATES-1992]

J. K. Bates, W. L. Ebert, X. Feng, and W. L. Bourcier, "Issues Affecting the Prediction of Glass Reactivity in an Unsaturated Environment," *J. Nucl. Mater.*, Vol. **190**, 198-227 (1992).

[KNAUSS-1990]

Knauss, K.G., W. L. Bourcier, K. D. McKeegan, C. I. Merzbacher, S. N. Nguyen, F. J. Ryerson, D. K. Smith, and H. C. Weed, "Dissolution Kinetics of a Simple Analogue Nuclear Waste Glass as a Function of pH, Time, and Temperature," *Mat. Res. Soc. Symp. Proc.*, Vol. **176**: 371-381 (1990).

[NIST-1991]

National Institute of Standards and Technology, Certificate, Standard Reference Material 185g, Potassium Hydrogen Phthalate, pH Standard, Feb. 13, 1991.

[NIST-1996]

National Institute of Standards and Technology, Standard Reference Materials, Potassium Dihydrogen Phosphate (186-I-f) and Disodium Hydrogen Phosphate (186-II-f), pH Primary Standards, Dec. 5, 1996.

[NIST-1998]

National Institute of Standards and Technology, Certificate, Standard Reference Material 187d, Sodium Tetraborate Decahydrate (Borax), pH Standard, Dec. 21, 1998.

[PEREIRA-1997]

Pereira, C., M. Hash, M. Lewis, and M. Richmann, 1997. "Ceramic-Composite Waste Forms from the Electrometallurgical Treatment of Spent Nuclear Fuel," *JOM* 34-37, July 1997.

[RORABACHER-1999]

Rorabacher, D. B., and A. Kandegedara, "Noncomplexing Tertiary Amines as "Better" Buffers Covering the range of pH 3-11. Temperature Dependence Their Acid Dissociation Constants." *Analytical Chemistry*. **71**, 3140-3144 (1999).

[TRW-1998]

TRW Environmental Safety Systems Inc., Total System Performance Assessment--Viability Assessment (TAPA-VA) Analyses Technical Basis Document, Chapter 6, "Waste Form degradation, Radionuclides Mobilization, and Transport Through the Engineered Barrier System," B00000000-01717-4301-00006 REV 01 (November 13, 1998).

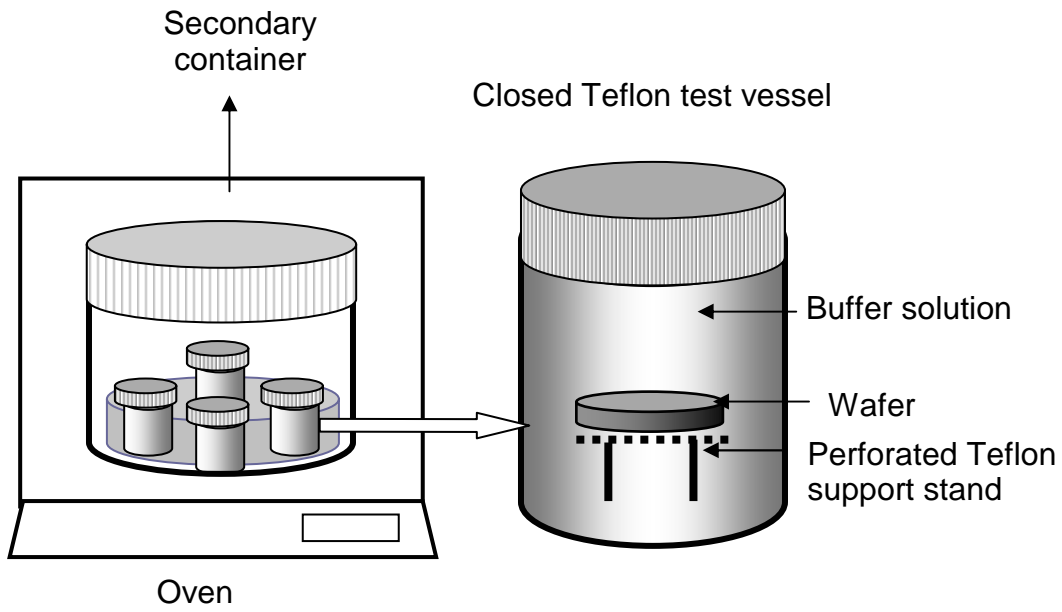


Fig. 1. Static Test Diagram

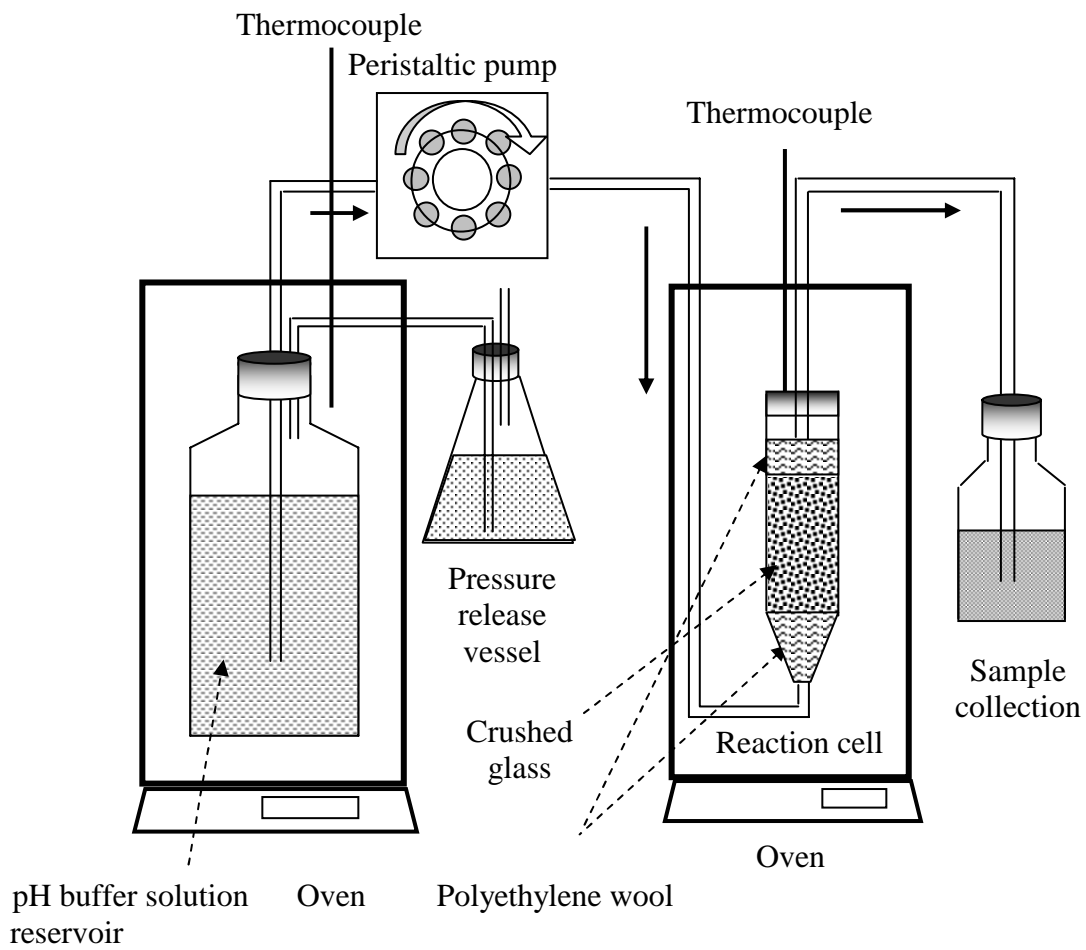


Fig. 2. Single-Pass Flow-Through Test Diagram

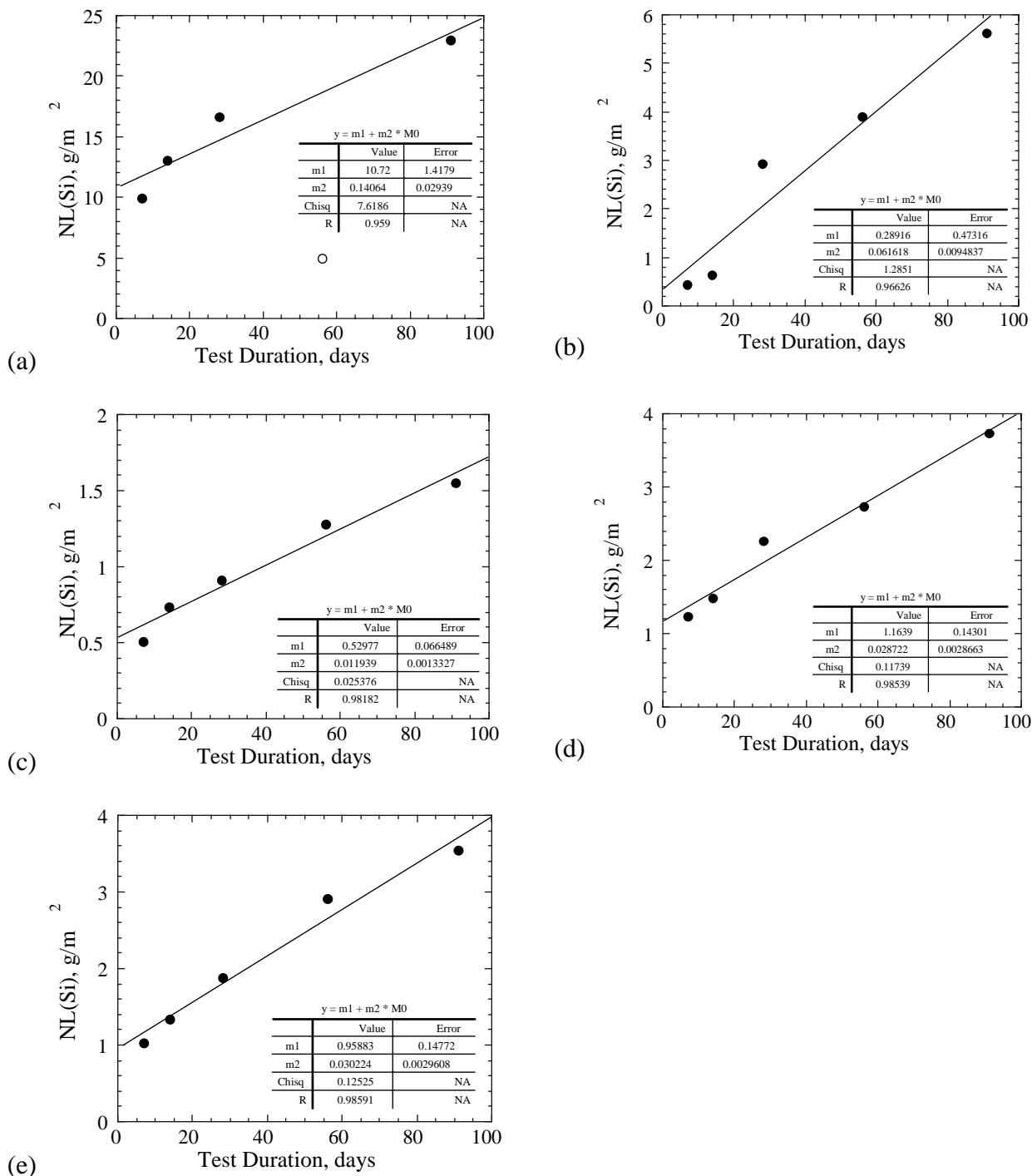


Fig. 3. Normalized Si Mass Losses [NL(Si)] from HIP Sodalite as a Function of Test Duration in Buffered Static Tests at 40°C. (a) Sodalite, pH 4.9, 40°C, (b) Sodalite, pH 6.0, 40°C, (c) Sodalite, pH 7.2, 40°C, (d) Sodalite, pH 8.3, 40°C, and (e) Sodalite, pH 9.6, 40°C. Open symbols represent data not used in the regression fits.

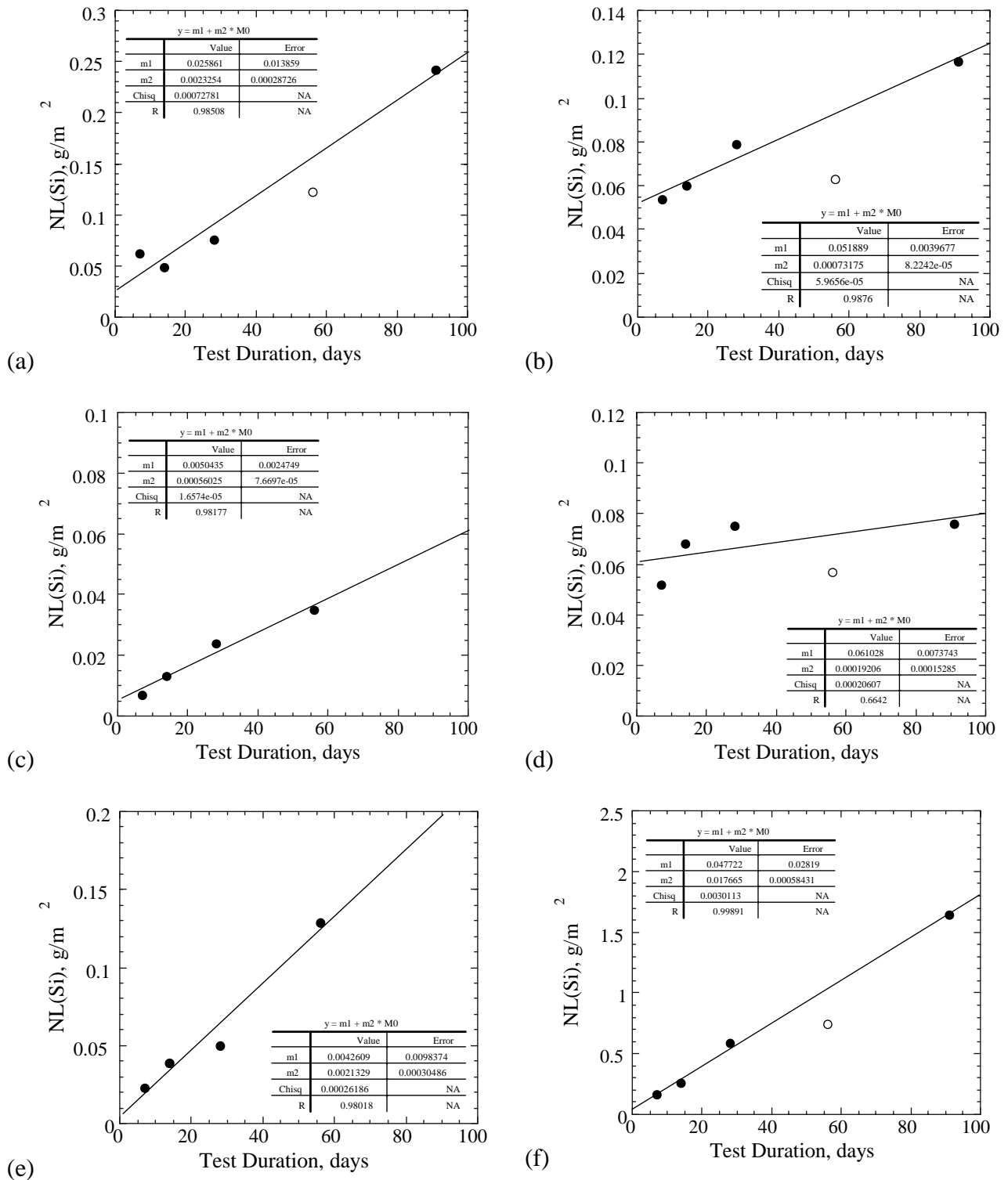


Fig. 4. Normalized Si Mass Losses [NL(Si)] from HIP Binder Glass as a Function of Test Duration in Buffered Static Tests at 40°C. (a) Binder Glass, pH 4.9, 40°C, (b) Binder Glass, pH 6.0, 40°C, (c) Binder Glass, pH 6.8, 40°C, (d) Binder Glass, pH 7.2, 40°C, (e) Binder Glass, pH 7.8, 40°C, and (f) Binder Glass, pH 8.3, 40°C. Open symbols represent data not used in the regression fits.

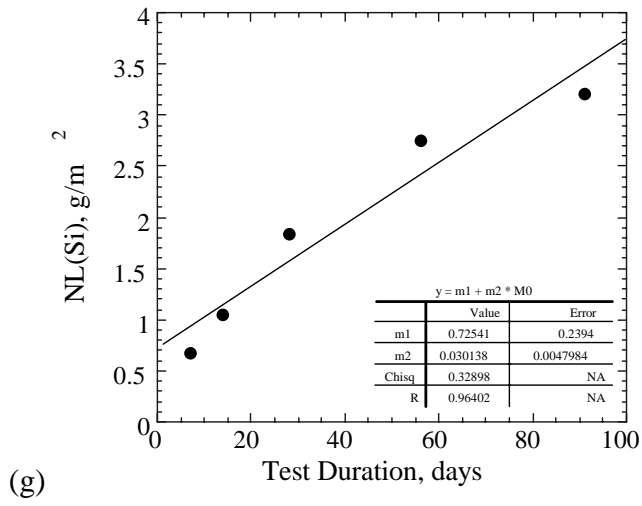


Fig. 4. (continued)

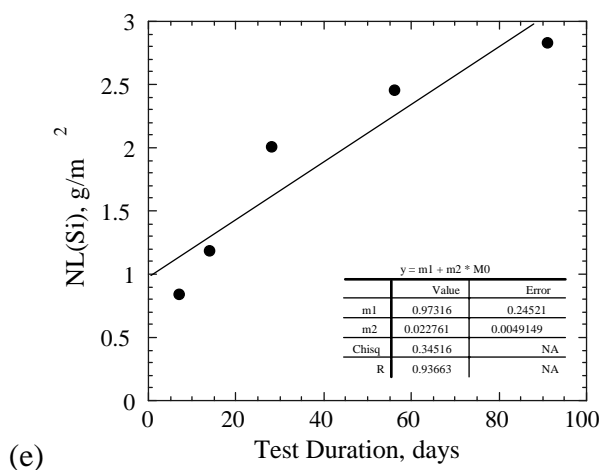
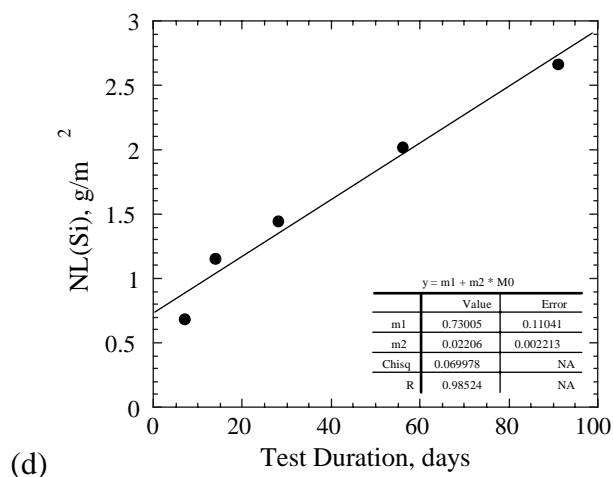
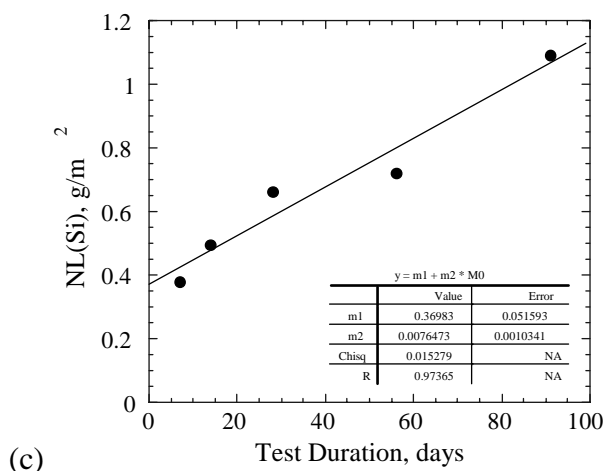
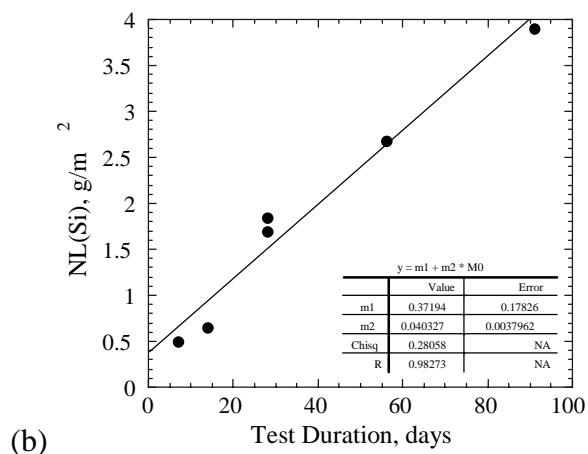
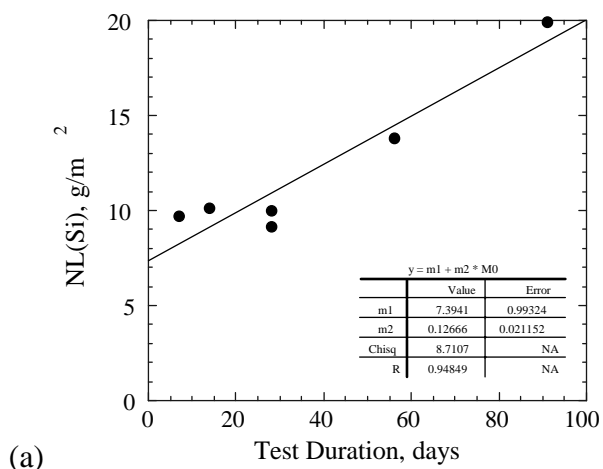


Fig. 5. Normalized Si Mass Losses [NL(Si)] from HIP CWF as a Function of Test Duration in Buffered Static Tests at 40°C. (a) CWF, pH 4.9, 40°C, (b) CWF, pH 6.0, 40°C, (c) CWF, pH 7.2, 40°C, (d) CWF, pH 8.3, 40°C, and (e) CWF, pH 9.6, 40°C.

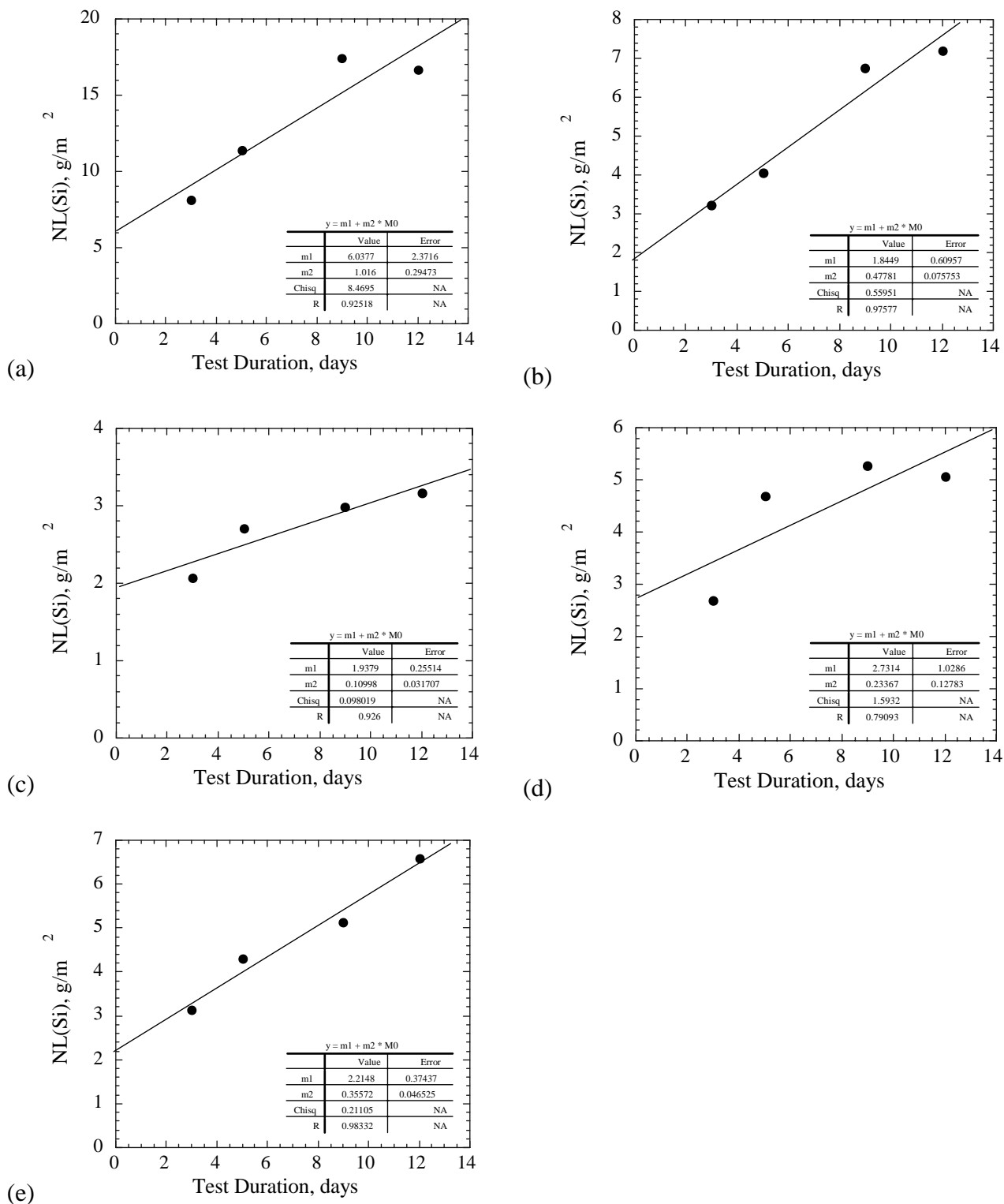


Fig. 6. Normalized Si Mass Losses [NL(Si)] from HIP Sodalite as a Function of Test Duration in Buffered Static Tests at 70°C. (a) Sodalite, pH 4.9, 70°C, (b) Sodalite, pH 6.4, 70°C, (c) Sodalite, pH 7.2, 70°C, (d) Sodalite, pH 8.3, 70°C, and (e) Sodalite, pH 9.4, 70°C.

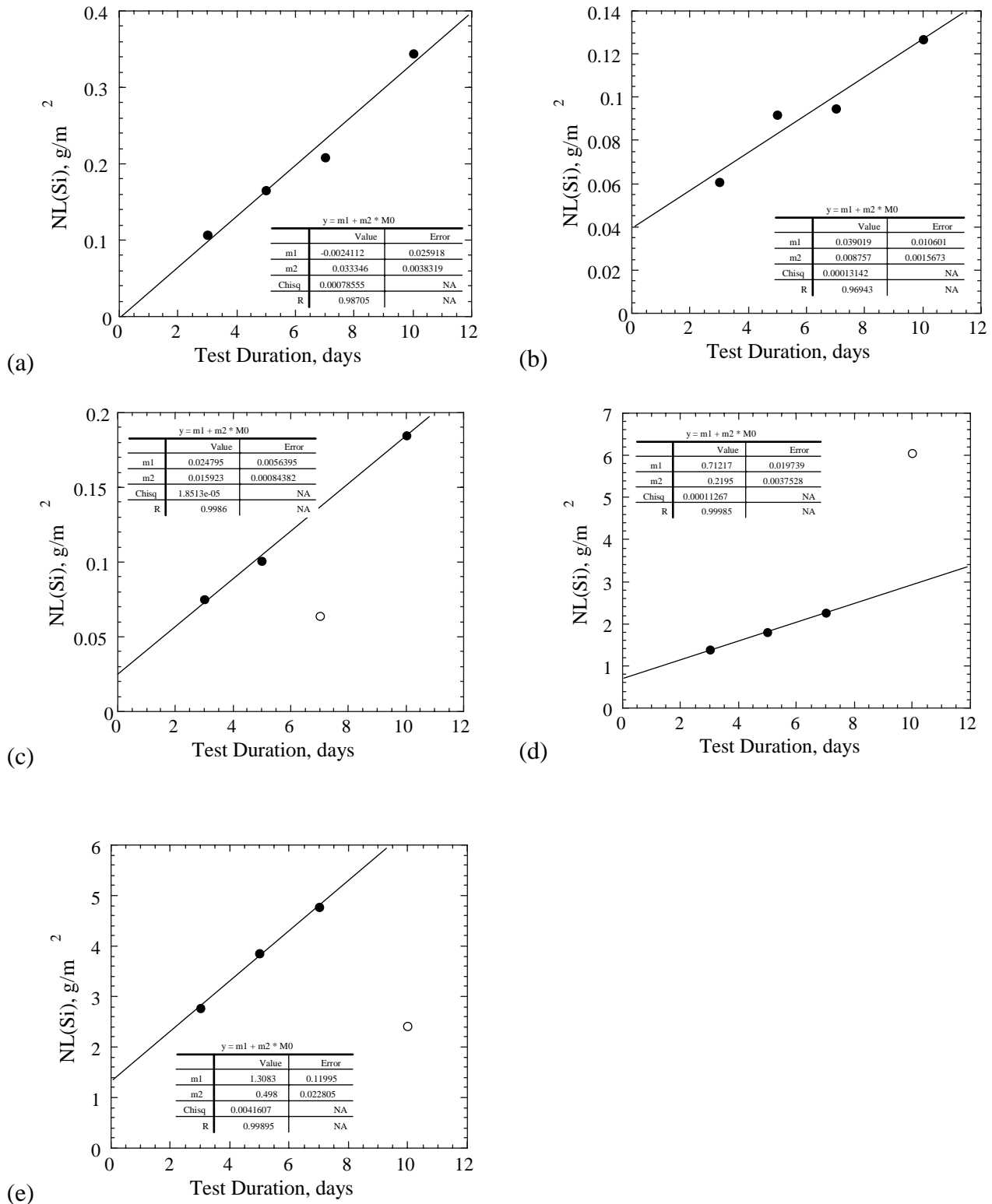


Fig. 7. Normalized Si Mass Losses [NL(Si)] from HIP Binder Glass as a Function of Test Duration in Buffered Static Tests at 70°C. (a) Binder Glass, pH 5.1, 70°C, (b) Binder Glass, pH 6.0, 70°C, (c) Binder Glass, pH 7.2, 70°C, (d) Binder Glass, pH 8.3, 70°C, and (e) Binder Glass, pH 9.6, 70°C. Open symbols represent data not used in the regression fits.

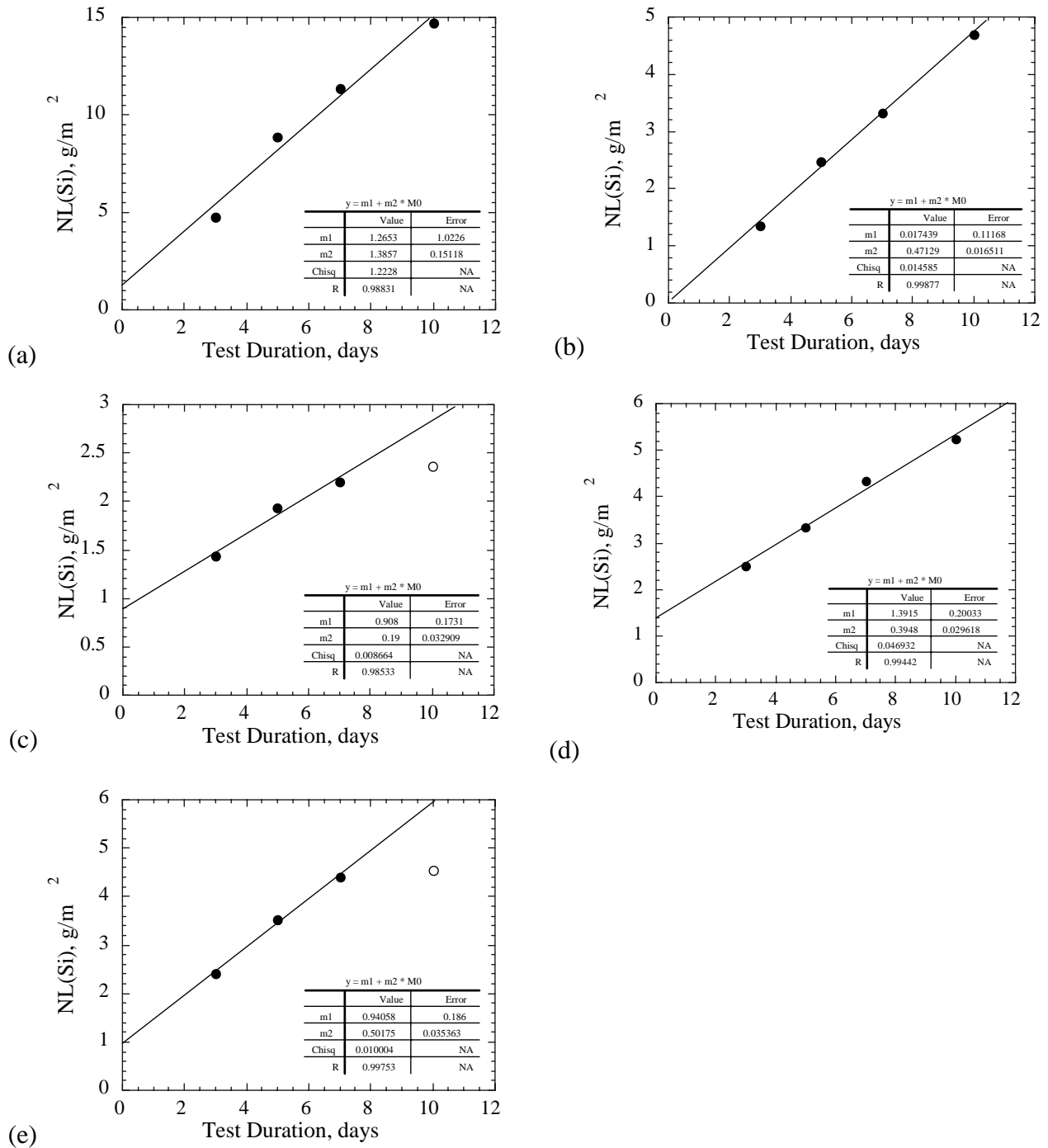


Fig. 8. Normalized Si Mass Losses [NL(Si)] from HIP CWF as a Function of Test Duration in Buffered Static Tests at 70°C. (a) CWF, pH 5.1, 70°C, (b) CWF, pH 6.0, 70°C, (c) CWF, pH 7.2, 70°C, (d) CWF, pH 8.3, 70°C, and (e) CWF, pH 9.6, 70°C. Open symbols represent data not used in the regression fits.

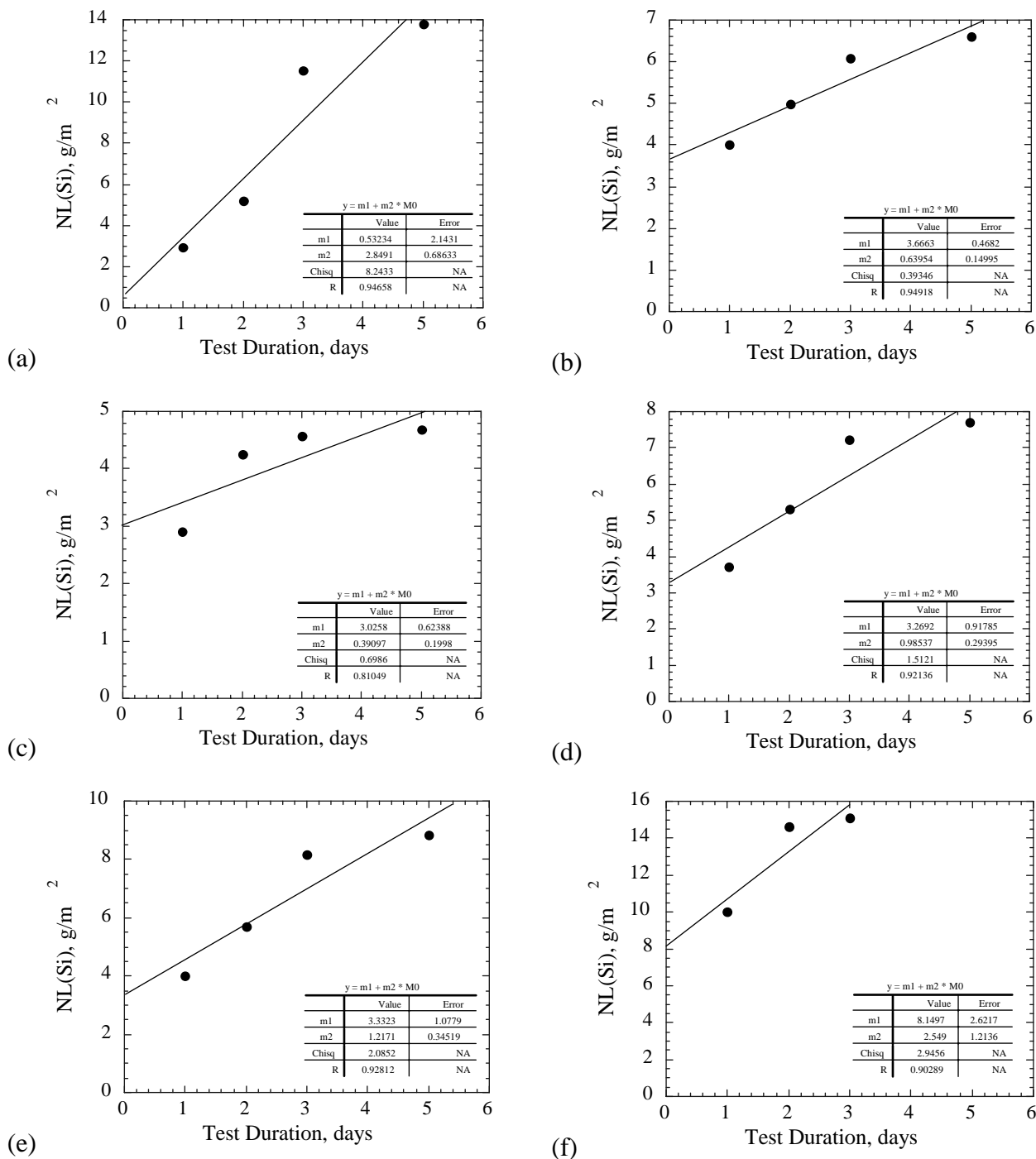


Fig. 9. Normalized Si Mass Losses [NL(Si)] from HIP Sodalite as a Function of Test Duration in Buffered Static Tests at 90°C. (a) Sodalite, pH 5.1, 90°C, (b) Sodalite, pH 6.0, 90°C, (c) Sodalite, pH 7.0, 90°C, (d) Sodalite, pH 8.1, 90°C, (e) Sodalite, pH 9.2, 90°C, and (f) Sodalite, pH 10.2, 90°C.

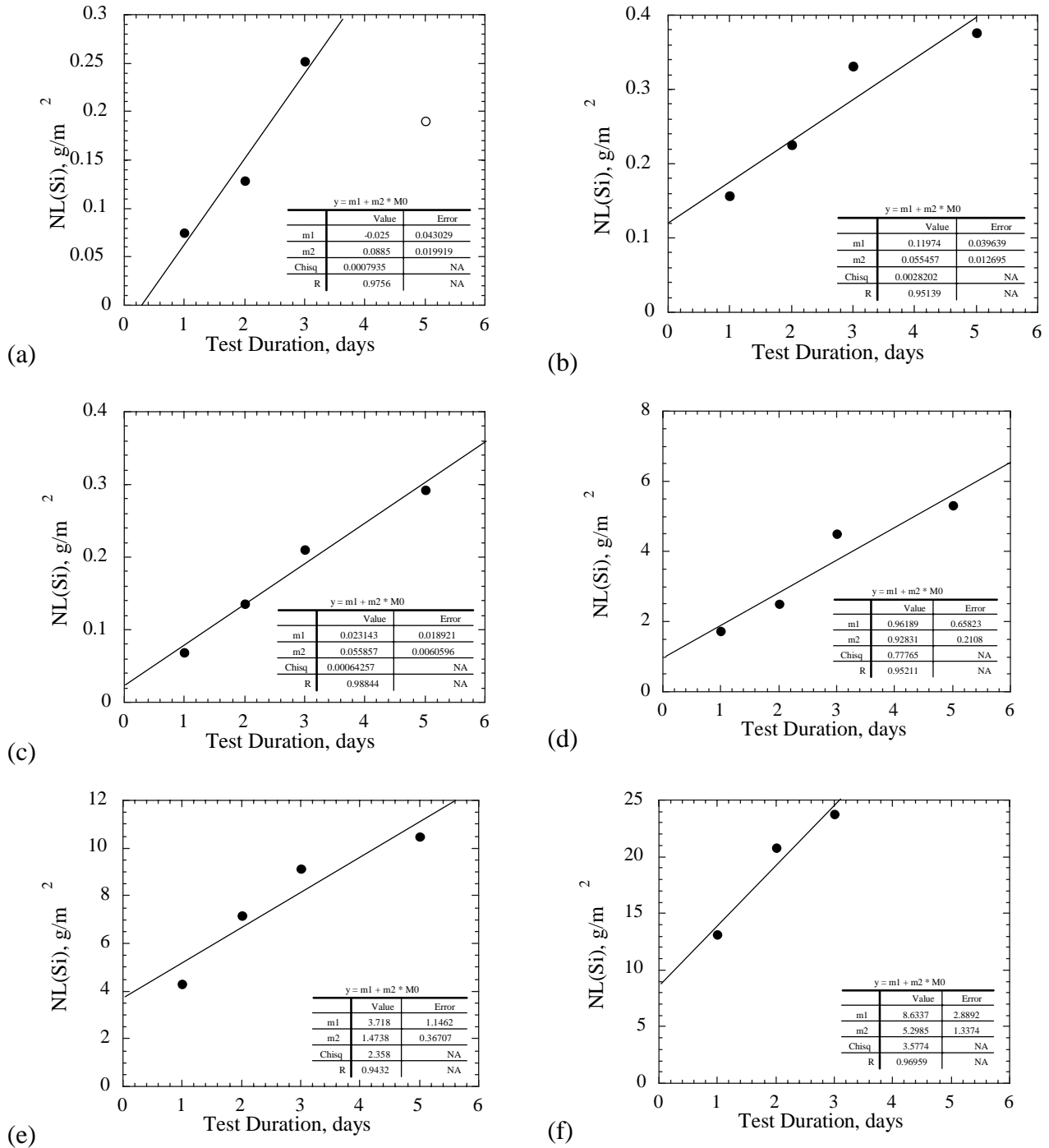


Fig. 10. Normalized Si Mass Losses [NL(Si)] from HIP Binder Glass as a Function of Test Duration in Buffered Static Tests at 90°C. (a) Binder Glass, pH 5.1, 90°C, (b) Binder Glass, pH 6.0, 90°C, (c) Binder Glass, pH 7.0, 90°C, (d) Binder Glass, pH 8.1, 90°C, (e) Binder Glass, pH 9.2, and 90°C, and (f) Binder Glass, pH 10.2, 90°C.

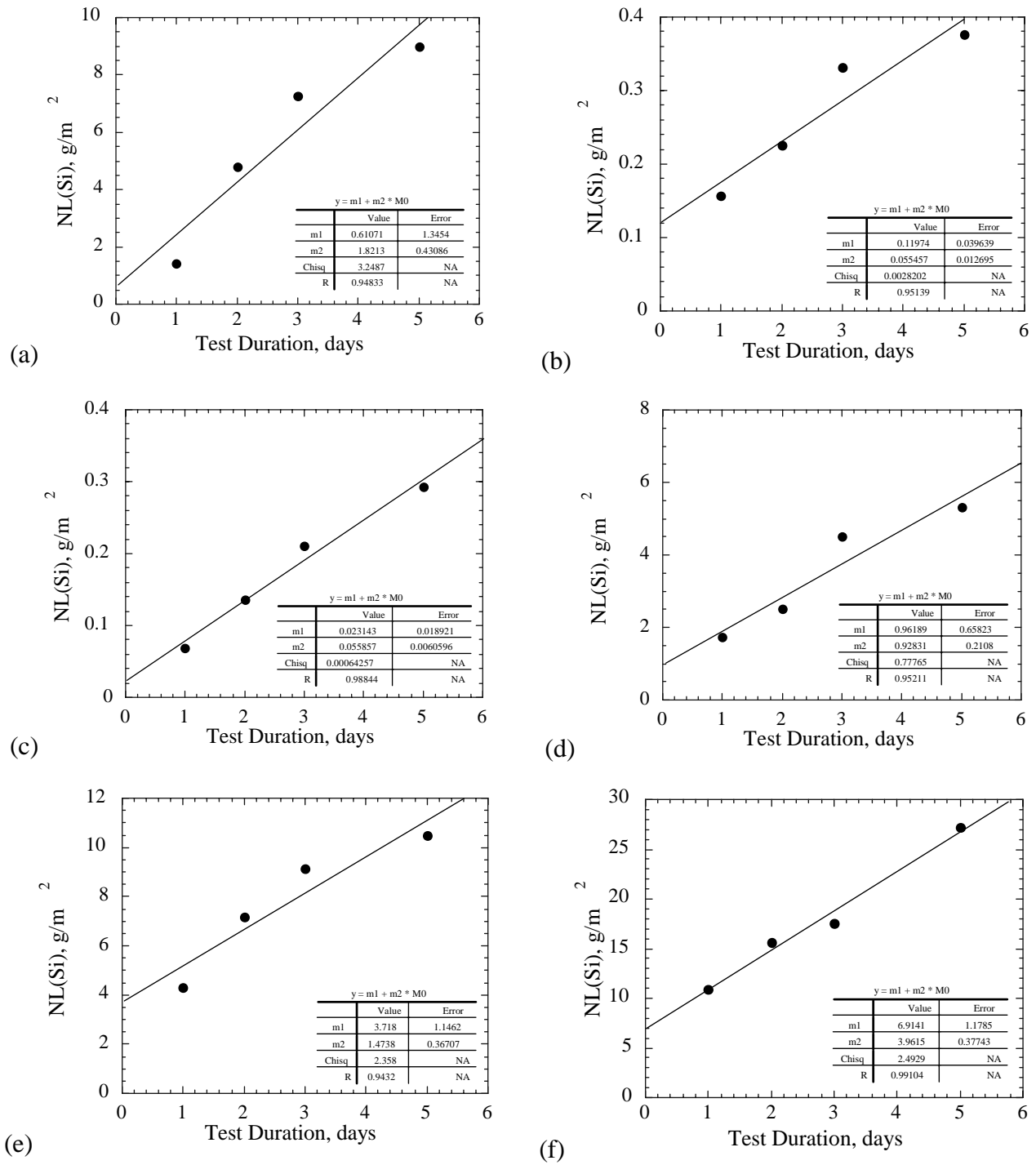
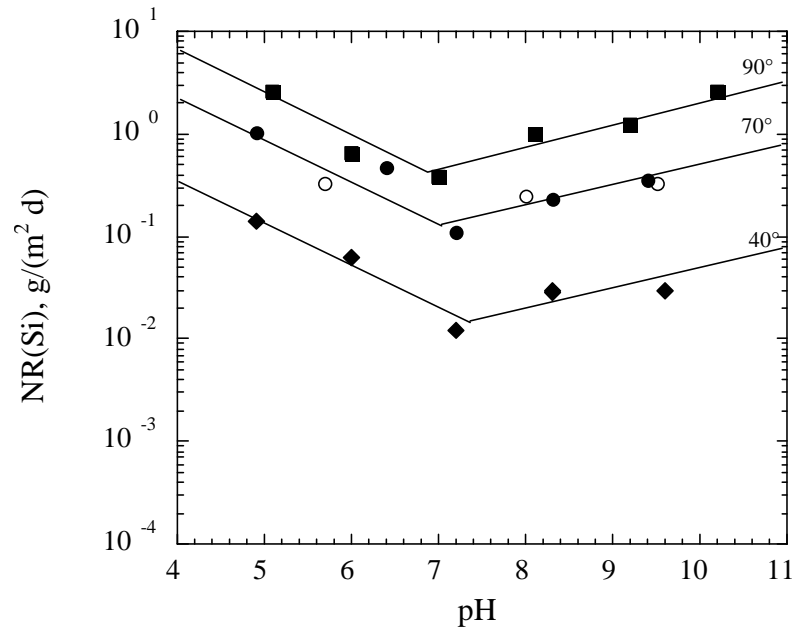
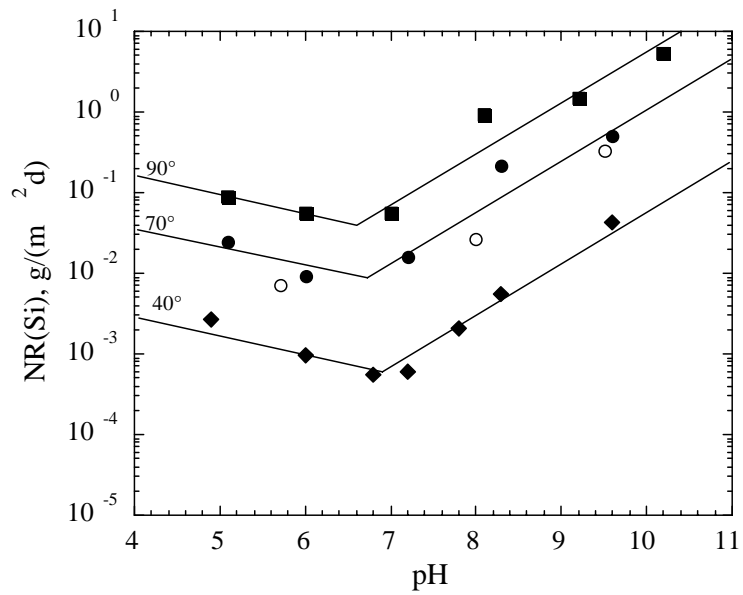


Fig. 11. Normalized Si Mass Losses [NL(Si)] from HIP CWF as a Function of Test Duration in Buffered Static Tests at 90°C. (a) CWF, pH 5.1, 90°C, (b) CWF, pH 6.0, 90°C, (c) CWF, pH 7.0, 90°C, (d) CWF, pH 8.1, 90°C, (e) CWF, pH 9.2, 90°C, and (f) CWF, pH 10.2, 90°C. Open symbols represent data not used in the regression fits.

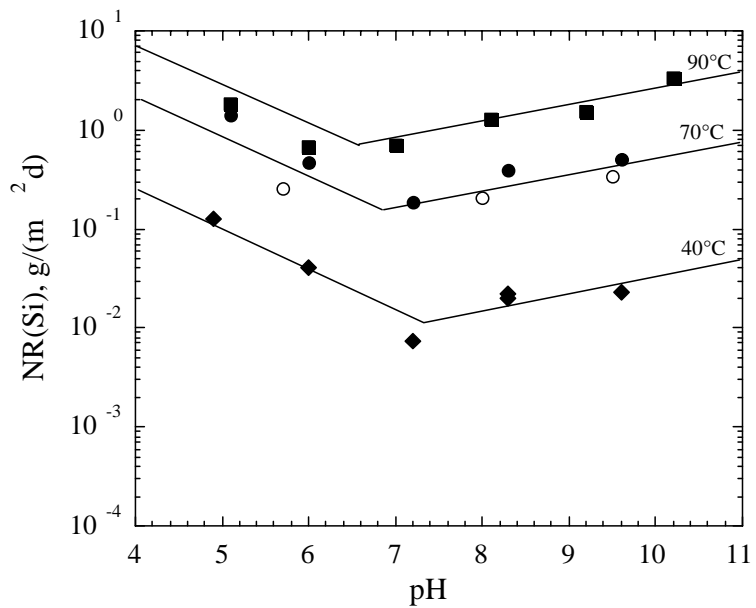


(a) HIP Sodalite



(b) HIP binder glass

Fig. 12. Temperature and pH Dependencies of NR(Si) from (a) Sodalite, (b) HIP Binder Glass, and (c) HIP CWF in Buffer Solutions. Rates measured in MES, PIPPS, and TEEN buffers at pH 5.7, 8.0, and 9.5 and 70°C are shown as open symbols.



(c) HIP CWF

Fig. 12. (continued)

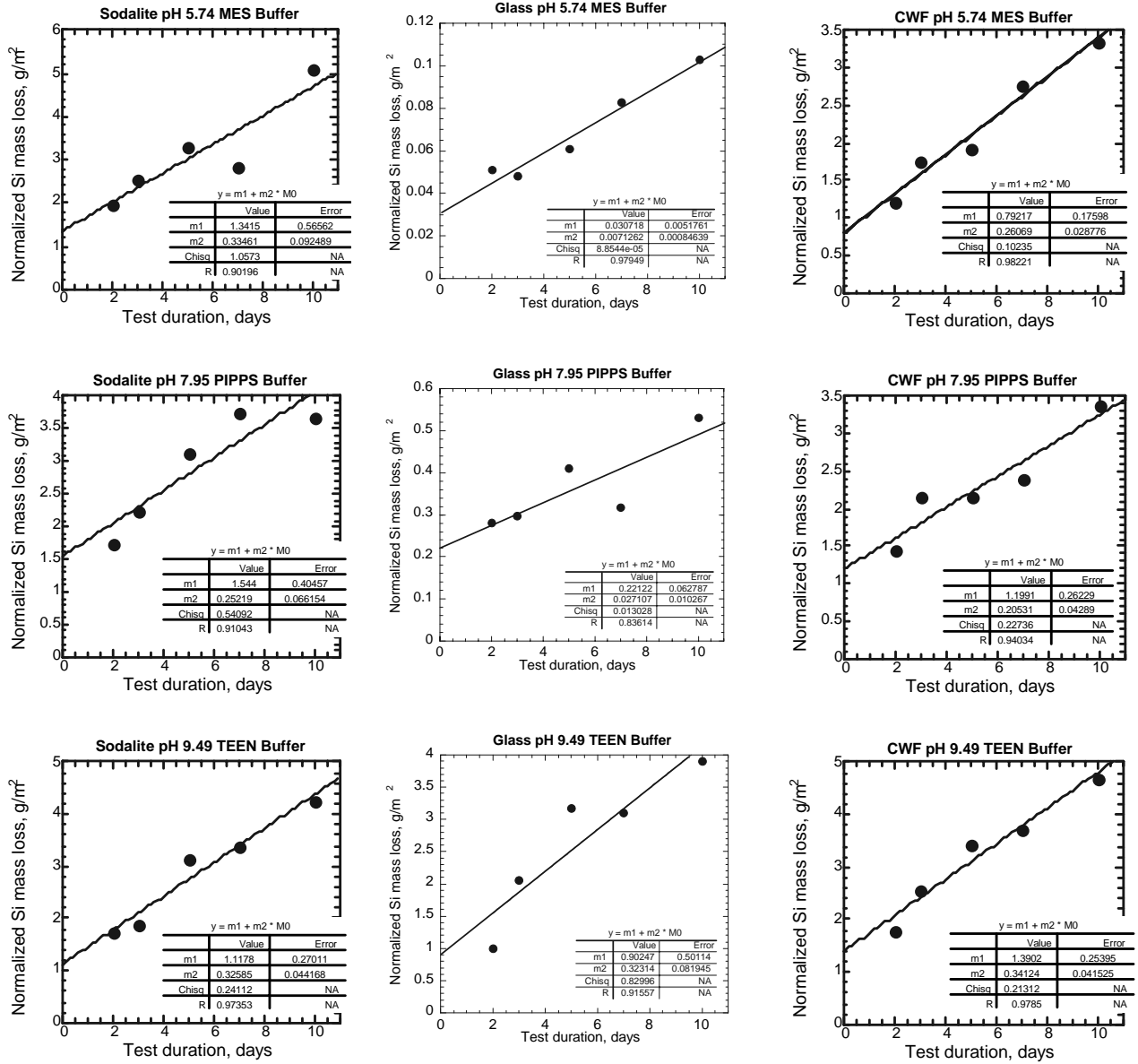
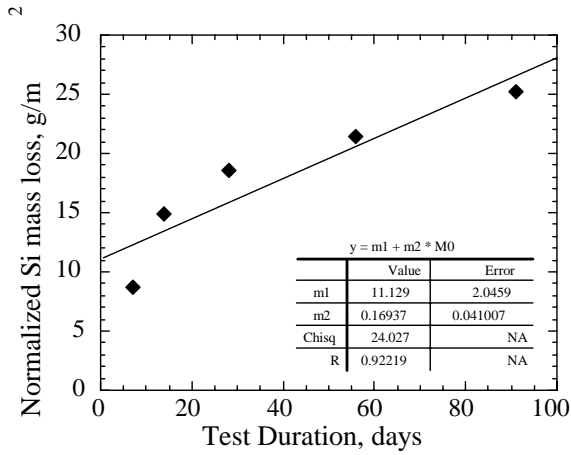
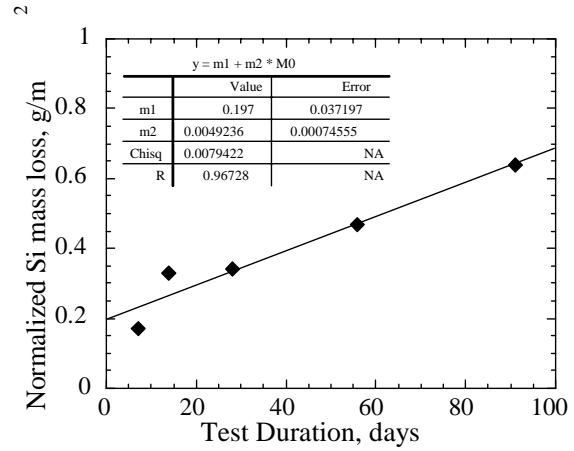


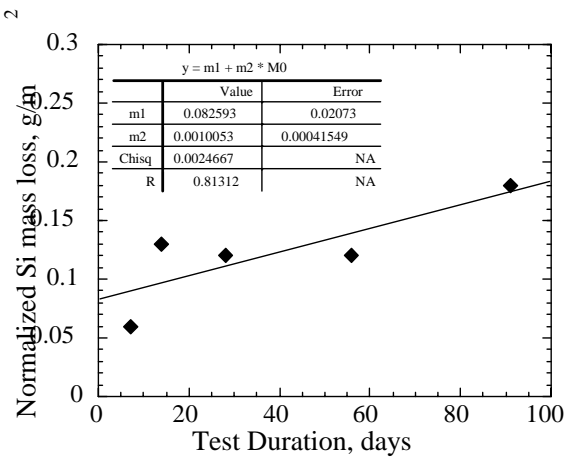
Fig. 13. NL(Si) for Static Tests with HIP Sodalite, Glass, and CWF in Noncomplexing Buffer Solutions at 70°C vs. Test Duration.



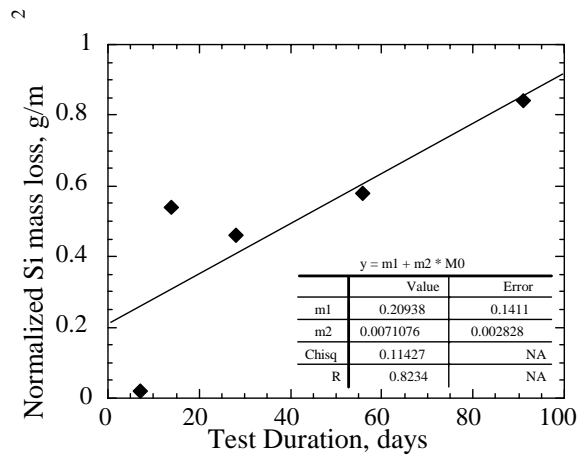
(a)



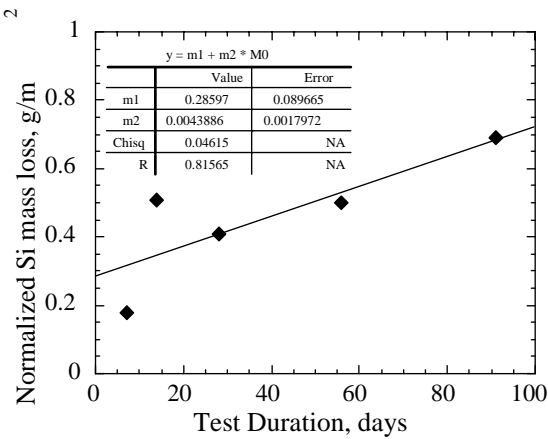
(b)



(c)

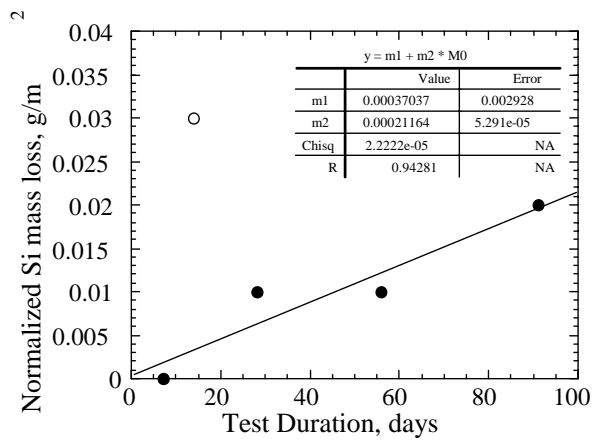


(d)

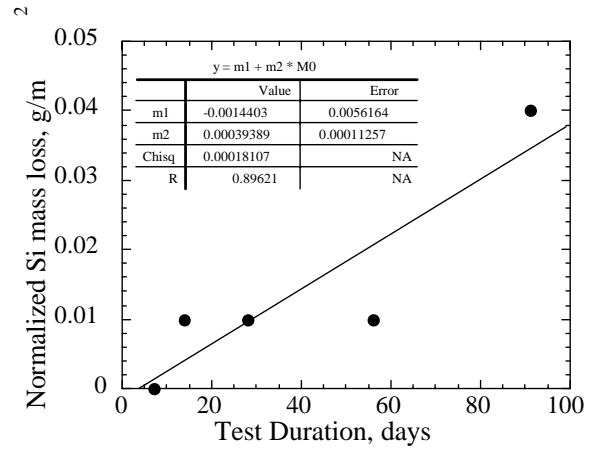


(e)

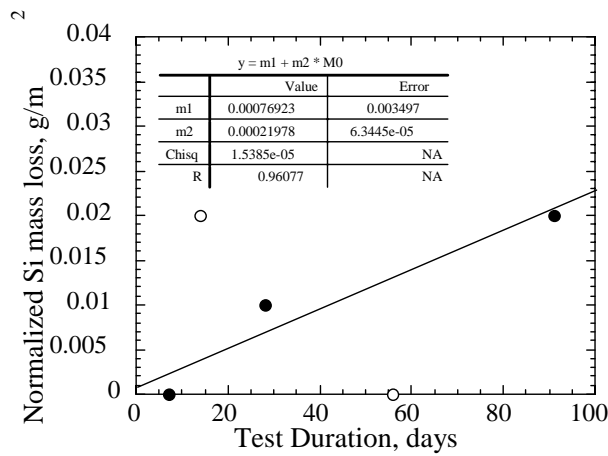
Fig. 14. Normalized Si Mass Losses from HIP Sodalite as a Function of Test Duration in Buffered Static Tests at 20°C. (a) HIP Sodalite, pH 4.8, 20°C, (b) HIP Sodalite, pH 6.1, 20°C, (c) HIP Sodalite, pH 7.3, 20°C, (d) HIP Sodalite, pH 8.3, and 20°C, and (e) HIP Sodalite, pH 9.8, 20°C.



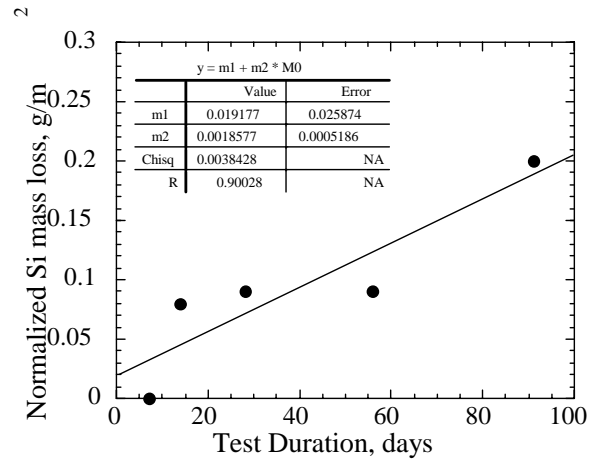
(a)



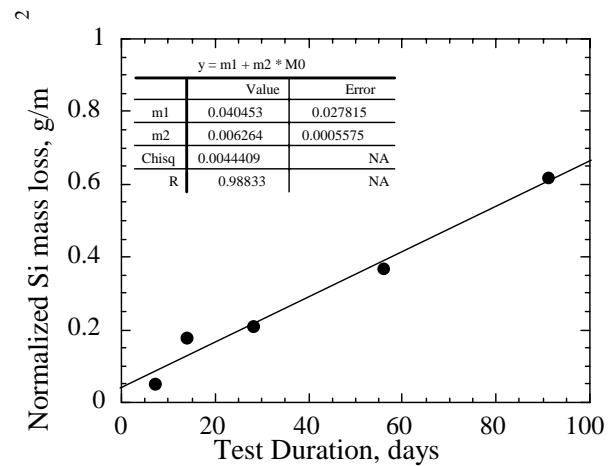
(b)



(c)

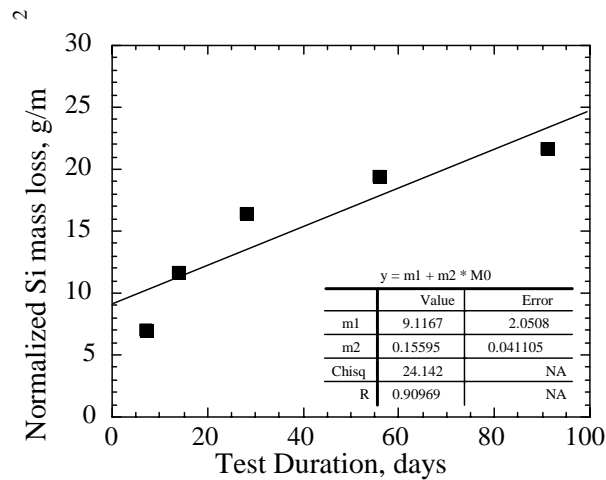


(d)

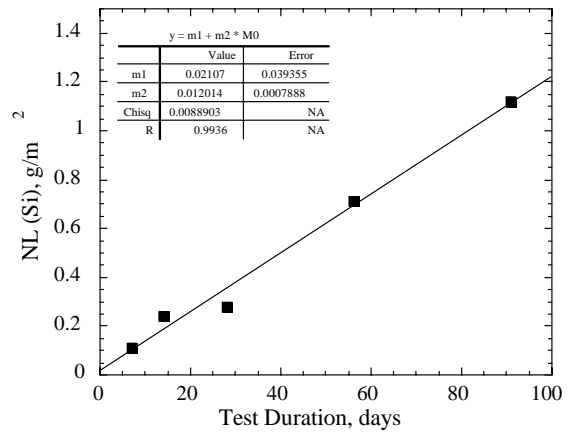


(e)

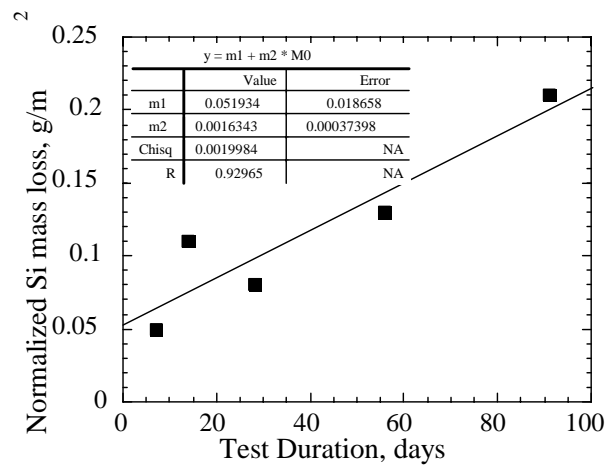
Fig. 15. Normalized Si Mass Losses from HIP Glass as a Function of Test Duration in Buffered Static Tests at 20°C (a) HIP Glass pH 4.8, 20°C, (b) HIP Glass, pH 6.1, 20°C, (c) HIP Glass, pH 7.3, 20°C, (d) HIP Glass, pH 8.3, 20°C, and (e) HIP Glass, pH 9.8, 20°C. Open circles represent data not used in the regression fits.



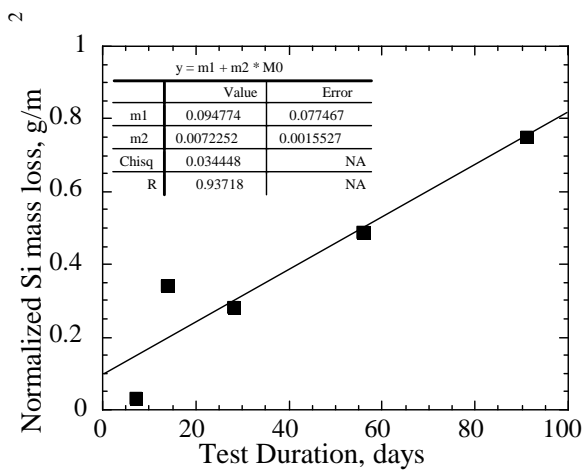
(a)



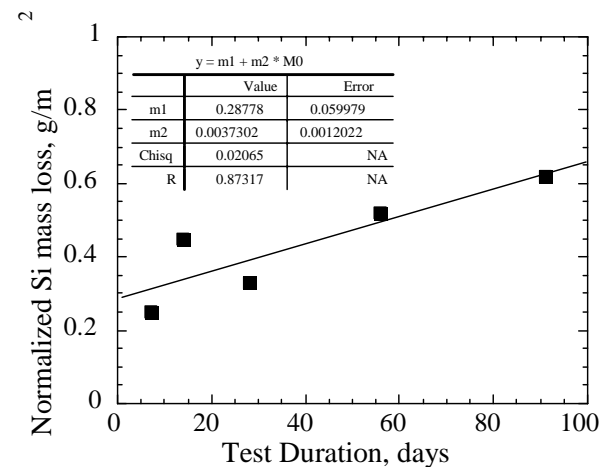
(b)



(c)

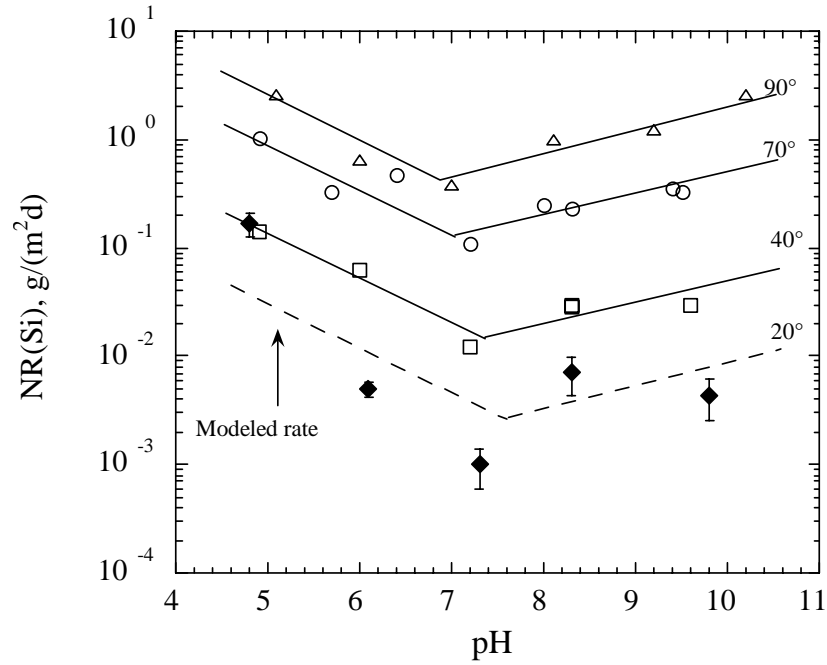


(d)

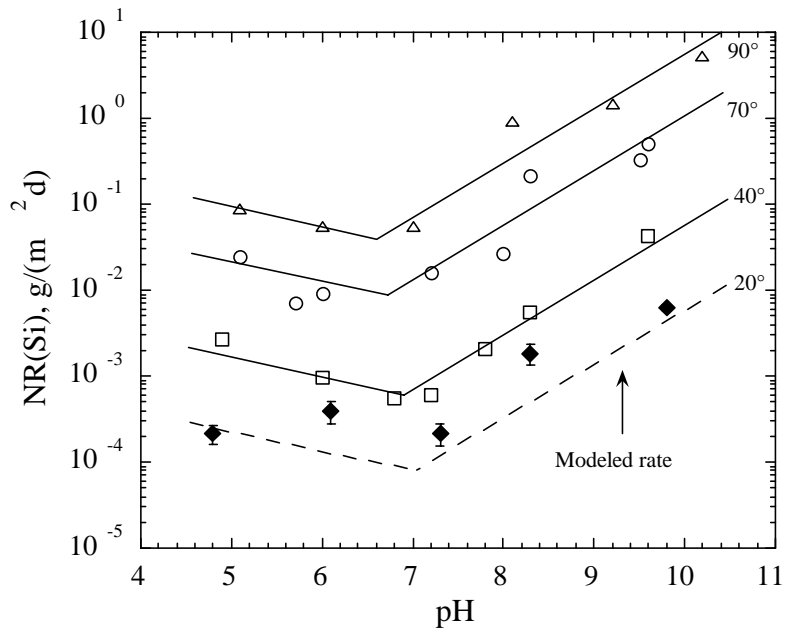


(e)

Fig. 16. Normalized Si Mass Losses from HIP CWF as a Function of Test Duration in Buffered Static Tests at 20°C. (a) HIP CWF, pH 4.8, 20°C, (b) HIP CWF, pH 6.1, 20°C, (c) HIP CWF, pH 7.3, 20°C, (d) HIP CWF, pH 8.3, 20°C, and (e) HIP CWF, pH 9.8, 20°C.

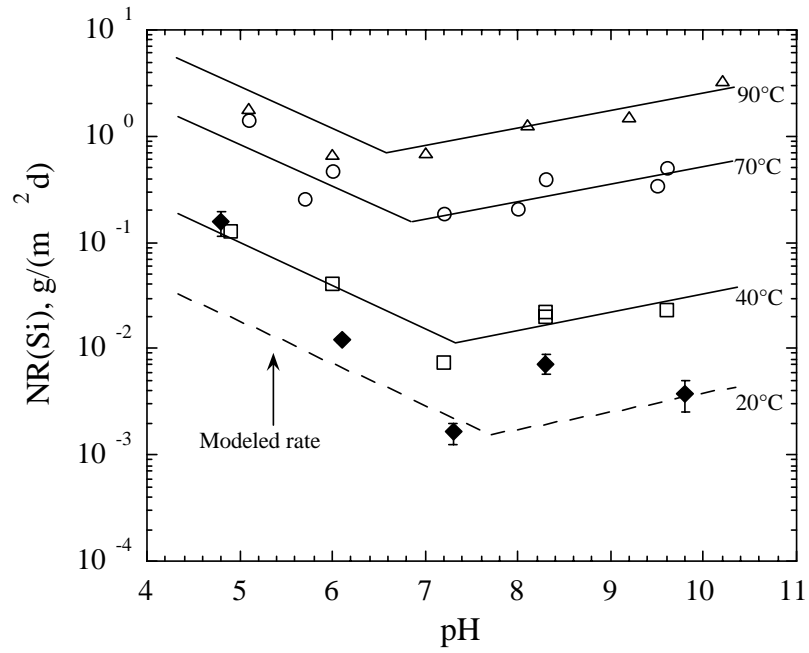


(a)



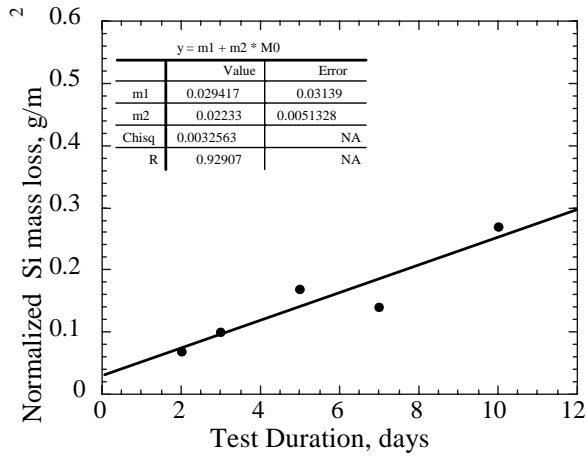
(b)

Fig. 17. Dissolution Rates as a Function of Temperature and pH for (a) Sodalite, (b) HIP Glass, and (c) HIP CWF. The V-shaped lines are calculated dissolution rates at 20, 40, 70, and 90°C using linear regression fits from dissolution rates at 40, 70, and 90°C.

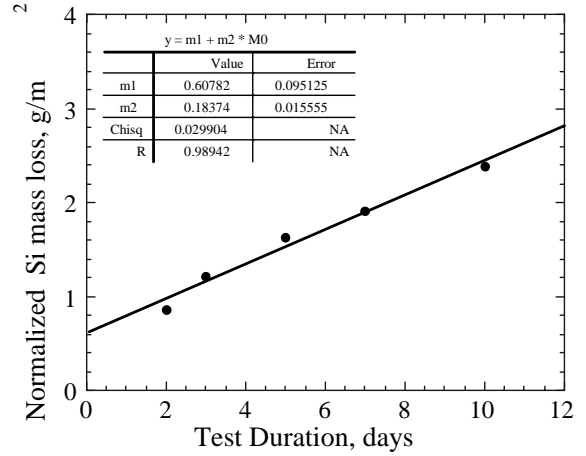


(c)

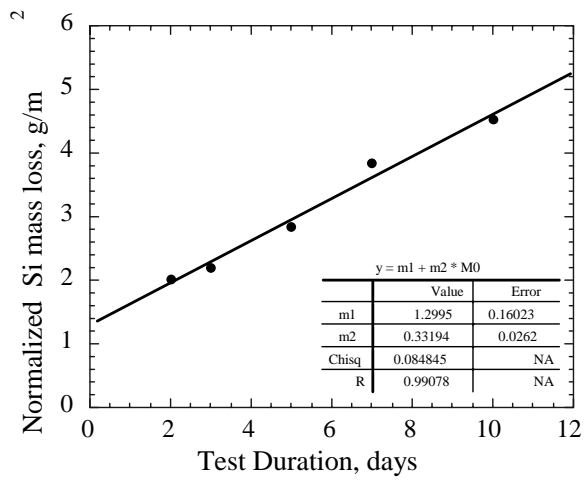
Fig. 17. (continued)



(a)

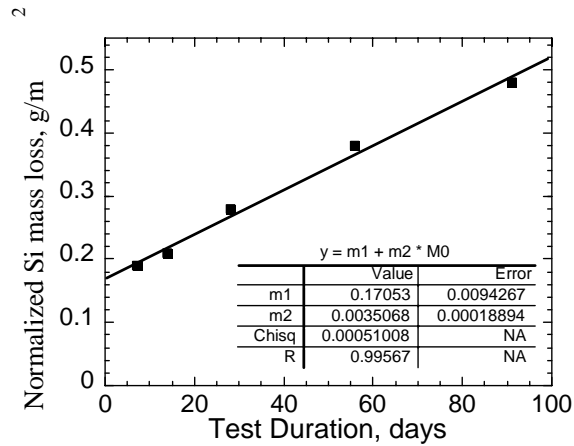


(b)

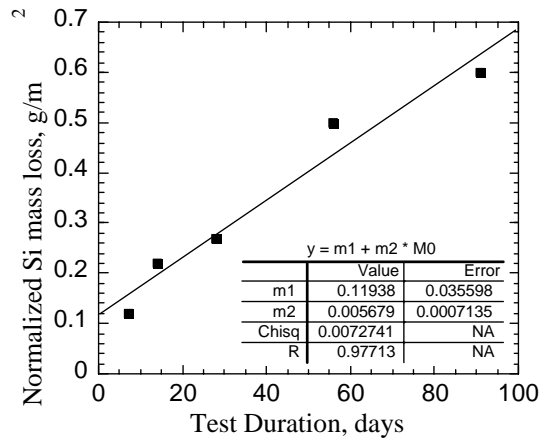


(c)

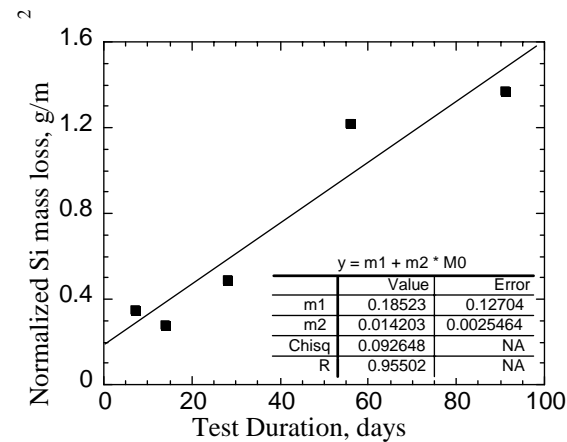
Fig. 18. Normalized Si Mass Losses from PC Binder Glass as a Function of Test Duration in Buffered Static Tests at 70°C. (a) pH 6.2, (b) pH 8.2, and (c) pH 9.5.



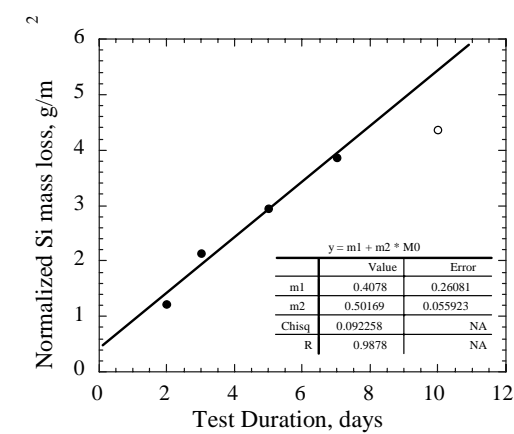
(a)



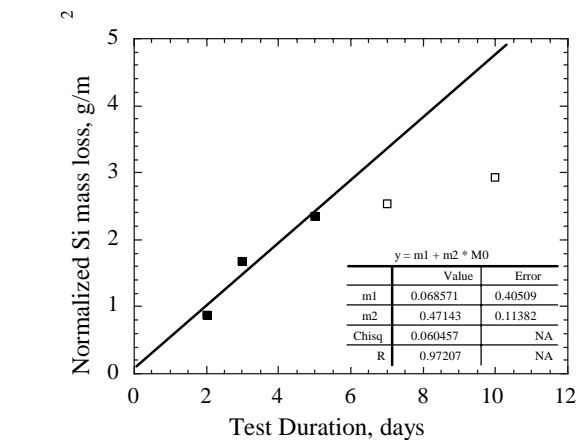
(b)



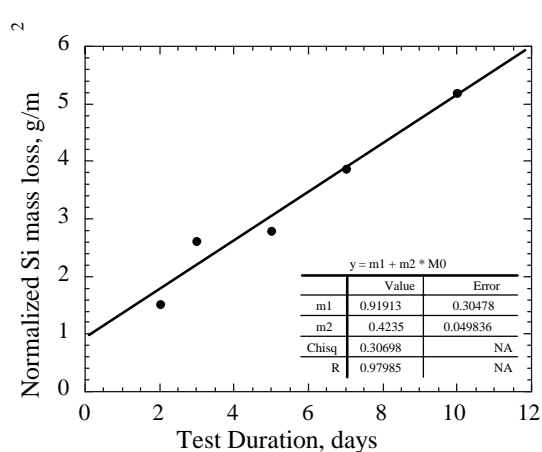
(c)



(d)

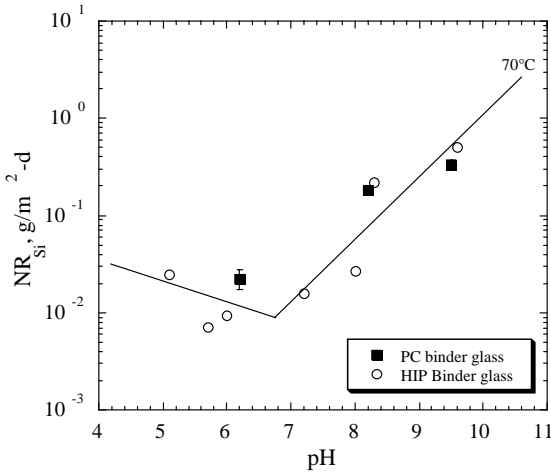


(e)

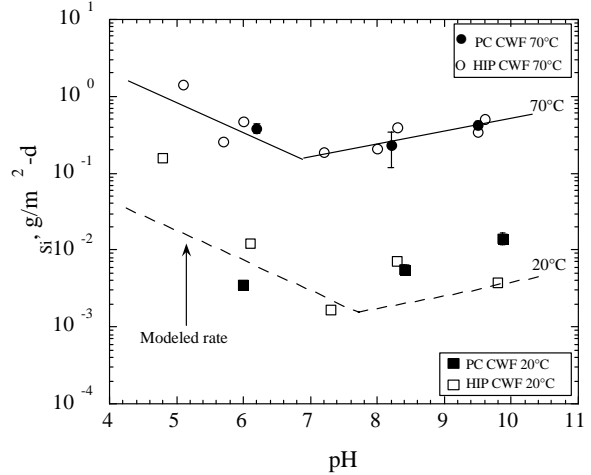


(f)

Fig. 19. Normalized Si Mass Losses from PC CWF as a Function of Test Duration in Buffer Static Tests at 20 and 70 °C. (a) 20 °C at pH 5.95, (b) 20 °C at pH 8.37, (c) 20 °C at pH 9.81, (d) 70 °C at pH 6.2, (e) 70 °C at pH 8.2, and (f) 70 °C at pH 9.5.

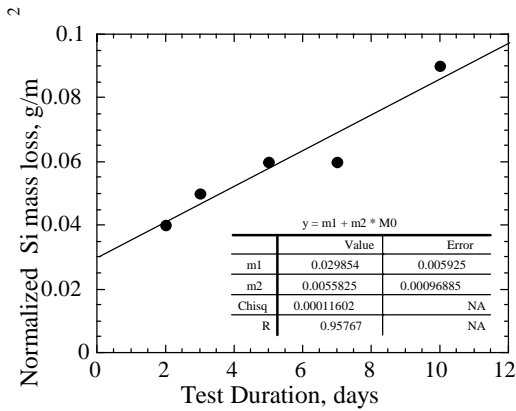


(a)

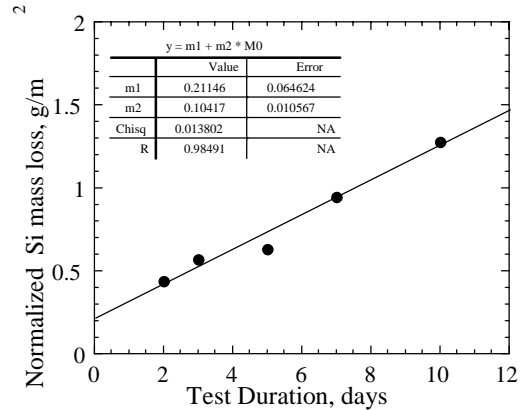


(b)

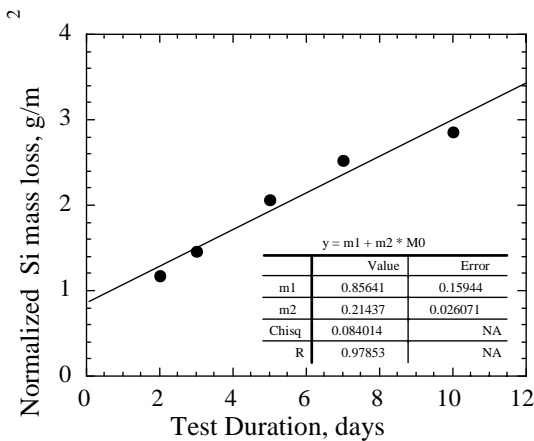
Fig. 20. Normalized Si Dissolution Rates as a Function of pH for (a) PC binder glass at 70°C and (b) PC CWF at 20 and 70°C. The lines are the modeled rates derived from (a) HIP binder glass at 40-90 °C and (b) HIP CWF at 40-90 °C.



(a) pH 6.2



(b) pH 8.2



(c) pH 9.5

Fig. 21. Normalized Si Mass Losses from Modified Glass as a Function of Test Duration in Buffered Static Tests at 70°C.

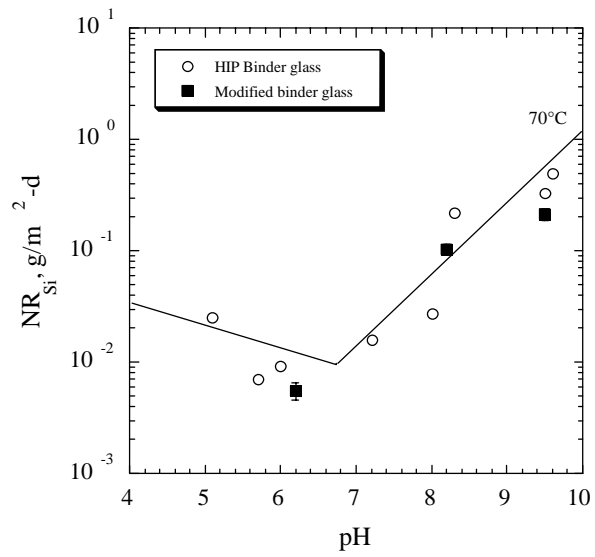
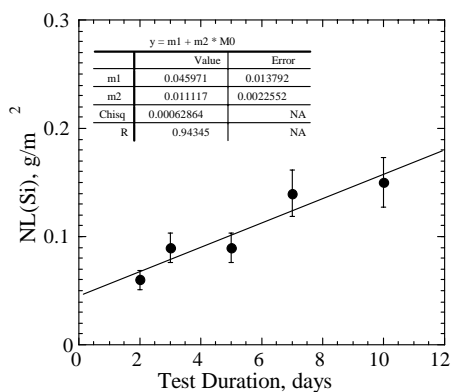
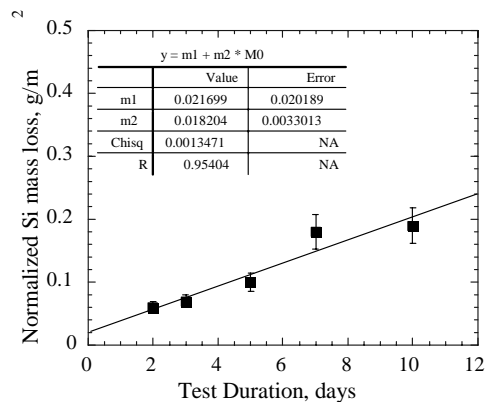


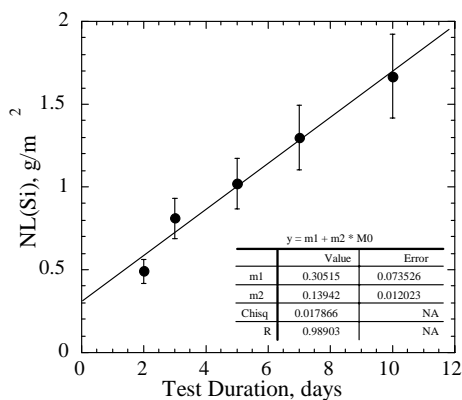
Fig. 22. Normalized Si Dissolution Rates as a Function of pH for modified Glass and HIP Binder Glass as a Function of Test Duration in Buffered Static Tests at $70^\circ C$.



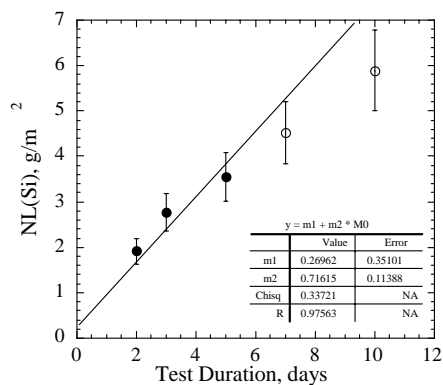
(a)



(b)



(c)



(d)

Fig. 23. Normalized Si Mass Losses as a Function of Test Duration from Static Tests on a Simple Five-Component Borosilicate Glass (CSG) in Buffer Solutions at 70°C. (a) pH 6.2, (b) pH 7.3, (c) pH 8.2, and (d) pH 9.5.

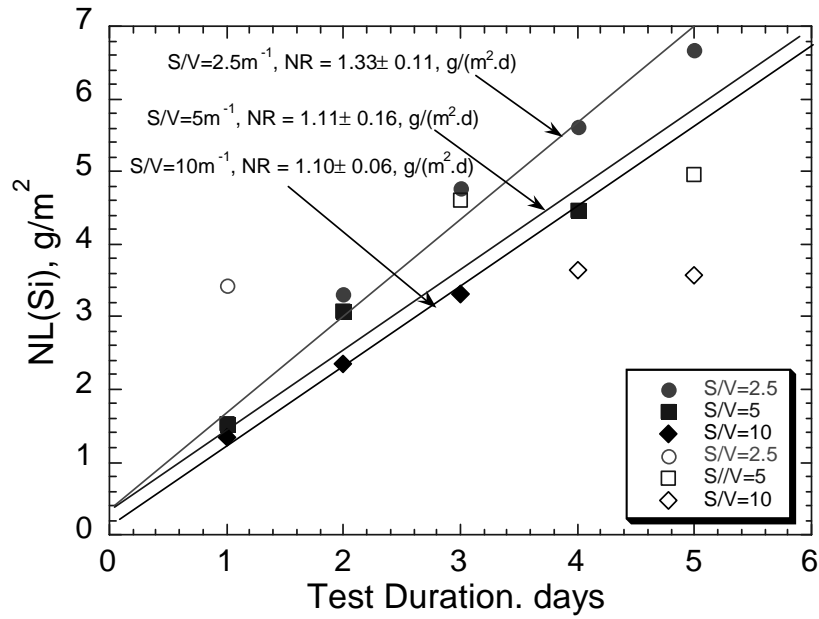
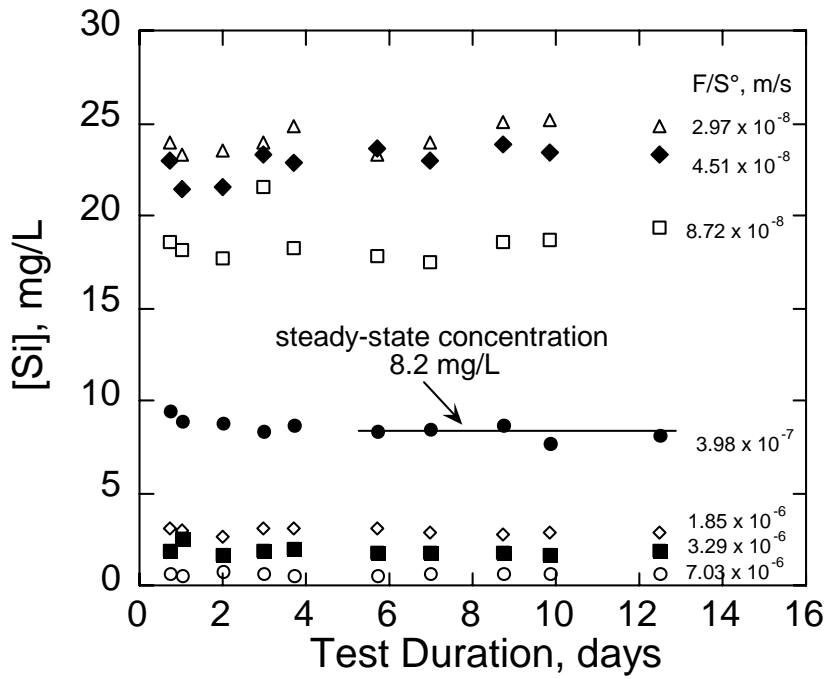
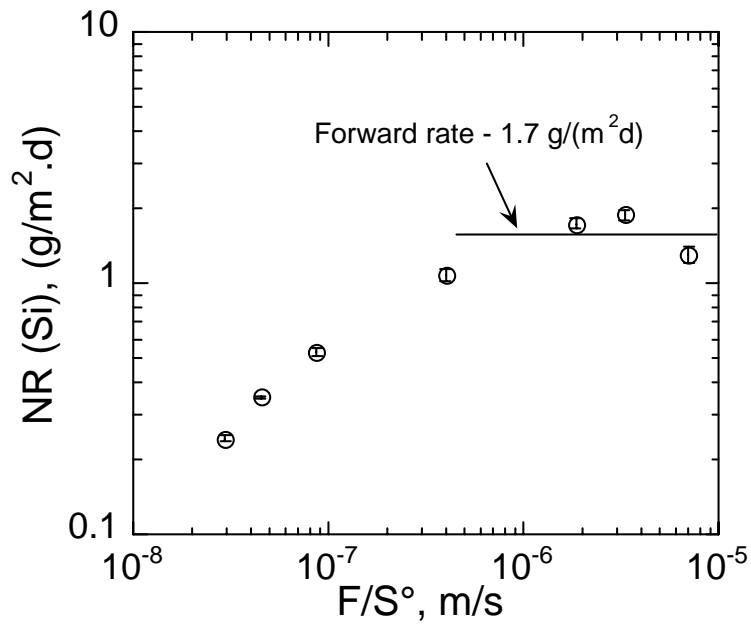


Fig. 24. Normalized Si Mass Losses as a Function of Test Duration from Static Tests on a CSG in Different S/V ratios (10, 5, and 2.5 m⁻¹) at 70°C. Open symbols represent data not used in the regression fits.

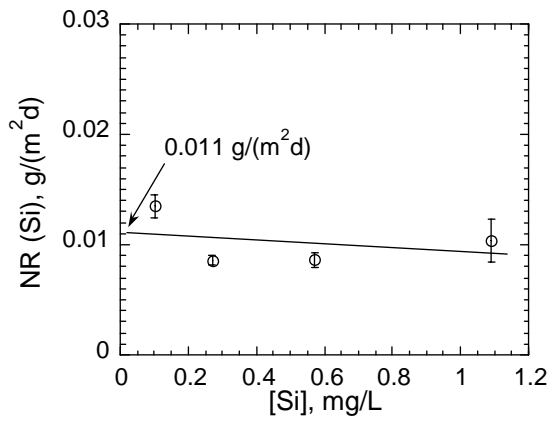


(a)

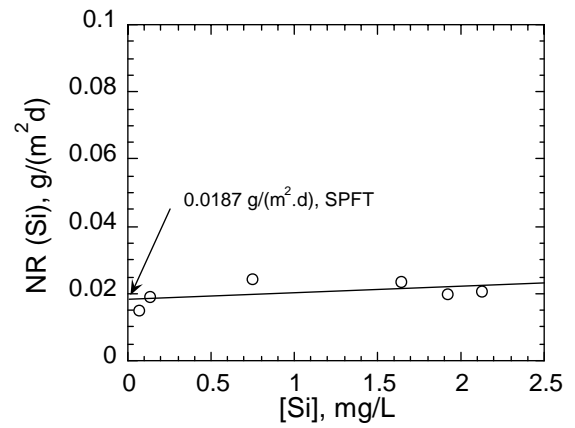


(b)

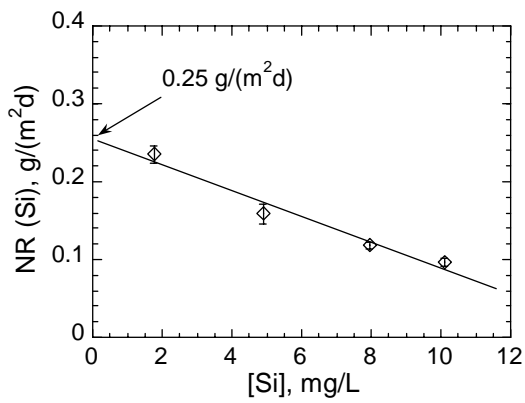
Fig. 25. Results of SPFT Tests with CSG Glass at pH 9.5 and 70 °C. (a) Si Concentration vs. Test Duration and (b) NR(Si) vs. F/S° .



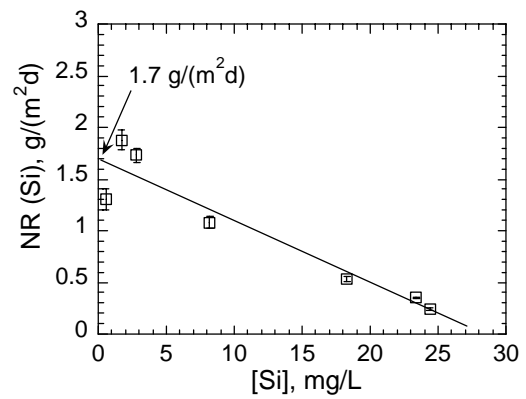
(a)



(b)



(c)



(d)

Fig. 26. NR(Si) vs. $C^{SS}(\text{Si})$ for SPFT Tests at 70°C. (a) pH 6.2, (b) pH 7.3, (c) pH 8.2, and (d) pH 9.5.

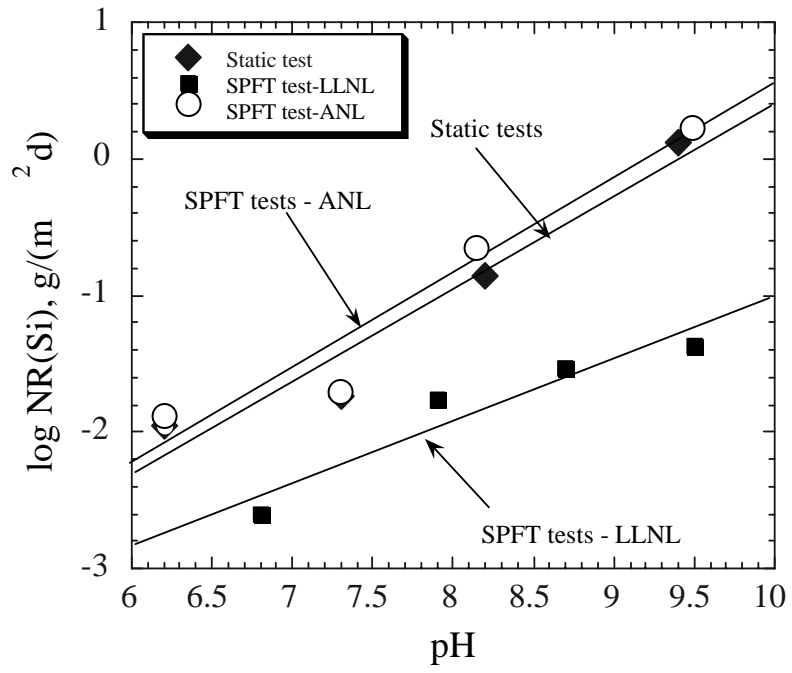


Fig. 27. NR(Si) vs. pH for Static and SPFT Tests at ANL and from KNAUSS [1990].

Table 1. Chemical Composition of CSG and Modified Glasses

Element	CSG Glass (wt%)		Modified glass (wt%)	
	Calc.	Measured	Calc.	Measured
B	3.86	3.63	6.52	6.40
Ca	2.42	2.48	4.79	4.16
Cl	4.85	4.74	0.75	0.74
Cs	-- ^a	--	1.27	0.18
K	--	--	0.04	0.02
Li	--	--	0.76	0.57
Na	--	--	0.12	0.10
Al	13.9	13.8	6.65	5.74
Si	27.7	26.9	26.9	28.0

^aNot present in glass.

Table 2. Compositions and Measured pH Values of Traditional Buffer Solutions at Test Temperatures

Buffer Composition	20°C	25°C	40°C	70°C	90°C
0.0095 m KHph + 0.0027 m LiOH ^a	4.84	4.86	4.96	5.03	5.18
0.0038 m KHph + 0.0031 m LiOH	5.95	5.87	5.99	6.20	6.25
0.0100 m HNO ₃ + 0.012 m TRIS ^b	7.35	7.51	7.14	6.57	6.29
0.064 m H ₃ BO ₃ + 0.010 m LiOH	8.37	8.39	8.31	8.27	8.14
0.012 m H ₃ BO ₃ + 0.010 m LiOH	9.81	9.84	9.68	9.56	9.37

^aKHph--potassium hydrogen phthalate

^bTRIS--tris(hydroxymethyl) aminomethane

Table 3. Properties of MES, PIPPS, and TEEN Buffers

Reagent	Full Name	-log (acid dissociation constant) [pK _a], 25°C
MES	2-(N-morpholino)ethanesulfonic acid	pK _{a1} 6.06 ± 0.10
PIPPS	Piperazine-N,N'-bis(3-propanesulfonic acid)	pK _{a2} 7.97 ± 0.01
TEEN	N,N,N,N'-tetraethylethylenediamine	pK _{a2} 9.88 ± 0.06

Table 4. Composition and Measured pH Values at 25, 40, and 70°C for Noncomplexing Buffers Used in Static Testing

Buffer Composition	pH at 25°C	pH at 40°C	pH at 70°C
0.0892 m MES + 0.0323 m LiOH	5.92	5.86	5.74
0.0019 m PIPPS + 0.0032 m LiOH	8.16	8.07	7.95
0.0909 m TEEN + 0.0165 m HNO ₃	10.40	10.12	9.49

Table 5 Normalized Dissolution Rates NR(Si) (g•m⁻²•d⁻¹) of HIP Sodalite, Binder Glass, and Ceramic Waste Form (CWF) as a Function of pH at 40, 70, and 90°C in Traditional and Noncomplexing Buffers.^a

40°C, Traditional Buffers				
Buffer	pH	NR(Si), (g/m ² •d)		
		Sodalite	Glass	CWF
KHph ^b -LiOH	4.9	0.14±0.03	0.0027±0.0003	0.127±0.021
KHph-LiOH	6.0	0.062±0.010	0.00096±0.00006	0.041±0.004
TRIS ^b -HNO ₃	6.8	–	0.00056±0.00008	–
TRIS-HNO ₃	7.2	0.012±0.001	0.00060±0.00015	0.0074±0.0010
Boric acid-LiOH	7.8	–	0.0021±0.0003	–
Boric acid-LiOH	8.3	0.029±0.003	0.0055±0.0039	0.022±0.002
Boric acid-LiOH	8.3	0.030±0.001	0.0056±0.0012	0.020±0.005
Boric acid-LiOH	9.6	0.030±0.003	0.043±0.0044	0.023±0.005
70°C, Traditional and Noncomplexing Buffers				
KHph-LiOH	4.9	1.02±0.29	–	–
KHph-LiOH	5.1	–	0.025±0.001	1.39±0.15
MES ^b -LiOH	5.7	0.33±0.09	0.0071±0.0009	0.26±0.03
KHph-LiOH	6.0	–	0.0093±0.0019	0.48±0.01
TRIS-HNO ₃	6.4	0.48±0.08	–	–
TRIS-HNO ₃	7.2	0.109±0.031	0.016±0.002	0.19±0.03
PIPPS ^b -LiOH	8.0	0.25±0.07	0.027±0.010	0.21±0.04
Boric acid-LiOH	8.3	0.23±0.13	0.22±0.004	0.40±0.03
Boric acid-LiOH	9.4	0.36±0.05	–	–
TEEN ^b -LiOH	9.5	0.33±0.04	0.33±0.08	0.34±0.04
Boric acid-LiOH	9.6	–	0.50±0.02	0.50±0.03
90°C, Traditional Buffers				
KHph-LiOH	5.1	2.6±0.6	0.088±0.020	1.82±0.43
KHph-LiOH	6.0	0.64±0.15	0.056±0.012	0.67±0.18
TRIS-HNO ₃	7.0	0.38±0.20	0.056±0.006	0.69±0.11
Boric acid-LiOH	8.1	0.98±0.29	0.93±0.21	1.29±0.13
Boric acid-LiOH	9.2	1.22±0.35	1.47±0.37	1.53±0.16
LiOH	10.2	2.6±1.2	5.3±1.3	3.3±0.8

^aUncertainties shown are standard errors from linear regression of NL(Si) vs. test duration.

^bReplicate tests. KHph - potassium hydrogen phthalate; TRIS - tris(hydroxymethyl)aminomethane; MES - 2-(N-morpholino)ethanesulfonic acid; PIPPS - piperazine-N,N'-bis(3-propanesulfonic acid); TEEN - N,N,N,N'-tetraethylethylenediamine.

Table 6. Regression Parameters for Acid and Base Legs Corresponding to Equation 8

	“Leg”	C_0	C_1	C_2	C_{pH}	C_T
Sodalite	Acid	-0.593±0.051	-0.418±0.060	-2911±297	6.040	0.002951
	Base	-0.736±0.028	0.208±0.029	-3587±162	8.485	0.002952
Binder Glass	Acid	-2.019±0.065	-0.229±0.093	-3978±357	5.844	0.002955
	Base	-1.211±0.062	0.630±0.064	-4544±348	8.450	0.002969
CWF	Acid	-0.596±0.074	-0.391±0.089	-3356±426	6.020	0.002951
	Base	-0.696±0.030	0.179±0.031	-4320±175	8.500	0.002952

^aFor sodalite and the CWF, measured dissolution rates in near-neutral pH are used in both the acid and base leg regression fits. For binder glass, only the pH = 6.8 results is used in both the acid and base leg regression fits.

Table 7. Model Parameters for Acid and Base Legs

Material	Leg	$\log k_0$	η	E_a
Sodalite	Acid	10.52±0.95	-0.418±0.060	55.7±5.7
	Base	8.09±0.54	0.208±0.029	68.7±3.1
Glass	Acid	11.07±1.19	-0.23±0.09	76.2±6.8
	Base	6.96±1.17	0.63±0.06	87.0±6.7
CWF	Acid	11.66±1.37	-0.39±0.09	64.3±8.2
	Base	10.53±0.58	0.179±0.03	82.7±3.4

APPENDIX A. MCC-1 TEST DATA AND NORMALIZED MASS LOSSES (NL_i)
FOR BUFFER TESTS

Table A.1. Results of Static Tests on HIP Sodalite in Buffer Solution at 40°C

pH	Duration (d)	S/V (m ⁻¹)	Concentration (µg Si/L)	NL (Si) (g/m ²)
4.9	7	10	16701	9.889
4.9	14	10	21990	13.051
4.9	28	10	27750	16.637
4.9	56	10	8580	5.002
4.9	91	10	38668	22.994
6.0	7	10	792	0.438
6.0	14	10	1126	0.638
6.0	28	10	4948	2.929
6.0	56	10	6581	3.902
6.0	91	10	9490	5.616
7.2	7	10	893	0.509
7.2	14	10	1267	0.732
7.2	28	10	1599	0.915
7.2	56	10	2209	1.280
7.2	91	10	2734	1.553
8.3	7	10	2837	1.232
8.3	14	10	3256	1.483
8.3	28	10	4726	2.267
8.3	56	10	5510	2.736
8.3	91	10	8423	3.731
9.6	7	10	1840	1.037
9.6	14	10	2353	1.343
9.6	28	10	3340	1.883
9.6	56	10	5065	2.917
9.6	91	10	6577	3.538

Table A.2. Results of Static Tests on HIP Binder Glass in Buffer Solution at 40°C

pH	Duration (d)	S/V (m ⁻¹)	Concentration (µg Si/L)	NL (Si) (g/m ²)
4.9	7	10	372	0.062
4.9	14	10	335	0.049
4.9	28	10	449	0.076
4.9	56	10	586	0.123
4.9	91	10	988	0.242
6.0	7	10	219	0.054
6.0	14	10	237	0.060
6.0	28	10	297	0.079
6.0	56	10	252	0.063
6.0	91	10	460	0.117
6.8	7	10	173	0.007
6.8	14	10	173	0.013
6.8	28	10	208	0.024
6.8	56	10	238	0.035
7.2	7	10	173	0.052
7.2	14	10	173	0.068
7.2	28	10	208	0.075
7.2	56	10	238	0.057
7.2	91	10	198	0.076
7.8	7	10	3145	0.023
7.8	14	10	1449	0.039
7.8	28	10	2539	0.050
7.8	56	10	2109	0.129
8.3	7	10	1275	0.168
8.3	14	10	1556	0.263
8.3	28	10	2670	0.586
8.3	56	10	3145	0.747
8.3	91	10	7053	1.647
9.6	7	10	2109	0.678
9.6	14	10	3225	1.056
9.6	28	10	5612	1.836
9.6	56	10	8322	2.754
9.6	91	10	10137	3.210

Table A.3. Results of Static Tests on HIP CWF in Buffer Solution at 40°C

pH	Duration (d)	S/V (m ⁻¹)	Concentration (µg Si/L)	NL (Si) (g/m ²)
4.9	7	10	19599	9.759
4.9	14	10	20314	10.114
4.9	28	10	18400	9.142
4.9	28	10	20114	9.996
4.9	56	10	27662	13.794
4.9	91	10	39916	19.931
6.0	7	10	1045	0.495
6.0	14	10	1358	0.652
6.0	28	10	3727	1.841
6.0	28	10	3430	1.692
6.0	56	10	5404	2.683
6.0	91	10	7874	3.902
7.2	7	10	796	0.378
7.2	14	10	1036	0.498
7.2	28	10	1388	0.662
7.2	56	10	1503	0.720
7.2	91	10	2310	1.090
8.3	7	10	2141	0.684
8.3	14	10	3075	1.154
8.3	28	10	3812	1.444
8.3	56	10	4955	2.020
8.3	91	10	7511	2.672
9.6	7	10	1789	0.844
9.6	14	10	2463	1.183
9.6	28	10	4203	2.013
9.6	56	10	5082	2.455
9.6	91	10	6307	2.832

Table A.4. Results of Static Tests on HIP Sodalite in Buffer Solution at 70°C

pH	Duration (d)	S/V (m ⁻¹)	Concentration (µg Si/L)	NL (Si) (g/m ²)
4.9	3	10	13500	8.130
4.9	5	10	18900	11.383
4.9	9	10	29000	17.431
4.9	12	10	26700	16.672
6.4	3	10	5350	3.219
6.4	5	10	6730	4.045
6.4	9	10	11200	6.764
6.4	12	10	11800	7.208
7.2	3	10	3530	2.075
7.2	5	10	4590	2.712
7.2	9	10	5030	2.983
7.2	12	10	5360	3.171
8.3	3	10	5100	2.678
8.3	5	10	8430	4.680
8.3	9	10	9420	5.277
8.3	12	10	9070	5.067
9.6	3	10	5320	3.129
9.6	5	10	7300	4.308
9.6	9	10	8680	5.141
9.6	12	10	11100	6.597

Table A.5. Results of Static Tests on HIP Binder Glass in Buffer Solution at 70°C

pH	Duration (d)	S/V (m ⁻¹)	Concentration (µg Si/L)	NL (Si) (g/m ²)
5.1	3	10	388	0.107
5.1	5	10	557	0.165
5.1	7	10	682	0.208
5.1	10	10	1140	0.344
6.0	3	10	252	0.061
6.0	5	10	375	0.092
6.0	7	10	349	0.095
6.0	10	10	448	0.127
7.2	3	10	443	0.075
7.2	5	10	519	0.101
7.2	7	10	410	0.064
7.2	10	10	766	0.185
8.3	3	10	4140	1.375
8.3	5	10	5390	1.801
8.3	7	10	6720	2.253
8.3	10	10	17900	6.055
9.6	3	10	8940	2.776
9.6	5	10	12100	3.851
9.6	7	10	14800	4.768
9.6	10	10	7890	2.416

Table A.6. Results of Static Tests on HIP CWF in Buffer Solution at 70°C

pH	Duration (d)	S/V (m ⁻¹)	Concentration (µg Si/L)	NL (Si) (g/m ²)
5.1	3	10	9610	4.766
5.1	5	10	17800	8.891
5.1	7	10	22600	11.336
5.1	10	10	29400	14.712
6.0	3	10	2760	1.361
6.0	5	10	4890	2.466
6.0	7	10	6630	3.327
6.0	10	10	9320	4.698
7.2	3	10	3070	1.440
7.2	5	10	4050	1.934
7.2	7	10	4580	2.200
7.2	10	10	4900	2.358
8.3	3	10	5080	2.514
8.3	5	10	6720	3.343
8.3	7	10	8690	4.337
8.3	10	10	10500	5.242
9.6	3	10	5390	2.405
9.6	5	10	7620	3.531
9.6	7	10	9320	4.412
9.6	10	10	9620	4.541

Table A.7. Results of Static Tests on HIP Sodalite in Buffer Solution at 90°C

pH	Duration (d)	S/V (m ⁻¹)	Concentration (µg Si/L)	NL (Si) (g/m ²)
5.1	1	10	4890	2.941
5.1	2	10	12600	5.182
5.1	3	10	18700	11.533
5.1	5	10	23000	13.813
6.0	1	10	6680	4.023
6.0	2	10	8300	4.993
6.0	3	10	10100	6.079
6.0	5	10	11000	6.605
7.0	1	10	4820	2.896
7.0	2	10	7070	4.252
7.0	3	10	7600	4.574
7.0	5	10	7790	4.682
8.1	1	10	6180	3.719
8.1	2	10	8810	5.299
8.1	3	10	12000	7.208
8.1	5	10	12800	7.690
9.2	1	10	6710	4.002
9.2	2	10	9470	5.696
9.2	3	10	13600	8.184
9.2	5	10	14700	8.835
10.2	1	10	16600	9.998
10.2	2	10	25000	14.649
10.2	3	10	25100	15.096

Table A.8. Results of Static Tests on HIP Binder Glass in Buffer Solution at 90°C

pH	Duration (d)	S/V (m ⁻¹)	Concentration (µg Si/L)	NL (Si) (g/m ²)
5.1	1	10	220	0.075
5.1	2	10	380	0.129
5.1	3	10	760	0.252
5.1	5	10	560	0.190
6.0	1	10	460	0.157
6.0	2	10	660	0.225
6.0	3	10	1000	0.331
6.0	5	10	1090	0.376
7.0	1	10	200	0.068
7.0	2	10	400	0.136
7.0	3	10	620	0.211
7.0	5	10	860	0.292
8.1	1	10	5120	1.739
8.1	2	10	7400	2.516
8.1	3	10	13300	4.503
8.1	5	10	15600	5.301
9.2	1	10	12700	4.321
9.2	2	10	21100	7.173
9.2	3	10	26800	9.120
9.2	5	10	30800	10.470
10.2	1	10	38700	13.160
10.2	2	10	61100	20.775
10.2	3	10	69900	23.757

Table A.9. Results of Static Tests on HIP CWF in Buffer Solution at 90°C

pH	Duration (d)	S/V (m ⁻¹)	Concentration (µg Si/L)	NL (Si) (g/m ²)
5.1	1	10	2830	1.428
5.1	2	10	9510	4.801
5.1	3	10	14400	7.261
5.1	5	10	17800	8.987
6.0	1	10	5630	2.846
6.0	2	10	7440	3.755
6.0	3	10	10100	5.096
6.0	5	10	10900	5.497
7.0	1	10	3660	1.849
7.0	2	10	5550	2.801
7.0	3	10	7520	3.807
7.0	5	10	9130	4.614
8.1	1	10	5360	2.704
8.1	2	10	8560	4.319
8.1	3	10	11800	5.955
8.1	5	10	15700	7.909
9.2	1	10	8520	4.221
9.2	2	10	12000	6.055
9.2	3	10	16500	8.101
9.2	5	10	19000	10.334
10.2	1	10	21700	10.955
10.2	2	10	30900	15.599
10.2	3	10	34700	17.497
10.2	5	10	53900	27.182

Table A.10. Results of Static Tests on Sodalite in Noncomplexing Buffer Solution at 70°C

pH	Duration (d)	S/V (m ⁻¹)	Concentration (µg Si/L)	NL (Si) (g/m ²)
5.74	2	10	3.3	1.984
5.74	3	10	4.26	2.563
5.74	5	10	5.44	3.279
5.93	7	10	4.67	2.8
5.74	10	10	8.47	5.109
7.95	2	10	2.88	1.73
7.95	3	10	3.74	2.254
7.95	5	10	5.16	3.114
7.51	7	10	6.22	3.749
7.95	10	10	6.11	3.68
9.49	2	10	2.92	1.724
9.49	3	10	3.14	1.855
9.49	5	10	5.53	3.153
9.36	7	10	5.92	3.399
9.49	10	10	7.33	4.252

Table A.11. Results of Static Tests on HIP Binder Glass in Noncomplexing Buffer Solution at 70°C

pH	Duration (d)	S/V (m ⁻¹)	Concentration (µg Si/L)	NL (Si) (g/m ²)
5.74	2	10	0.17	0.051
5.74	3	10	0.16	0.048
5.74	5	10	0.2	0.061
5.93	7	10	0.26	0.083
5.74	10	10	0.32	0.103
7.95	2	10	0.83	0.281
7.95	3	10	0.88	0.298
7.95	5	10	1.22	0.41
7.51	7	10	0.85	0.318
7.95	10	10	1.57	0.531
9.49	2	10	2.98	0.996
9.49	3	10	6.09	2.059
9.49	5	10	9.57	3.175
9.36	7	10	9.47	3.107
9.49	10	10	11.8	3.9

Table A.12. Results of Static Tests on HIP CWF in Noncomplexing Buffer Solution at 70°C

pH	Duration (d)	S/V (m ⁻¹)	Concentration (µg Si/L)	NL (Si) (g/m ²)
5.74	2	10	2.4	1.205
5.74	3	10	3.5	1.765
5.74	5	10	3.78	1.681
5.93	7	10	5.45	2.76
5.74	10	10	6.62	3.357
7.95	2	10	2.83	1.442
7.95	3	10	4.26	2.155
7.95	5	10	4.3	2.127
7.51	7	10	4.75	2.387
7.95	10	10	6.69	3.387
9.49	2	10	3.58	1.778
9.49	3	10	5.11	2.558
9.49	5	10	7	3.401
9.36	7	10	7.63	3.715
9.49	10	10	9.58	4.706

Table A.13. Results of Static Tests on Sodalite in Buffer Solution at 20°C

pH	Duration (d)	S/V (m ⁻¹)	Concentration (µg Si/L)	NL (Si) (g/m ²)
4.8	7	10	16500	8.74
4.8	14	10	27900	14.83
4.8	28	10	34900	18.58
4.8	56	10	40200	21.39
4.8	91	10	47500	25.30
6.1	7	10	378	0.17
6.1	14	10	673	0.33
6.1	28	10	699	0.34
6.1	56	10	934	0.47
6.1	91	10	1260	0.64
7.3	7	10	183	0.06
7.3	14	10	317	0.13
7.3	28	10	280	0.12
7.3	56	10	332	0.12
7.3	91	10	448	0.18
8.3	7	10	465	0.02
8.3	14	10	1440	0.54
8.3	28	10	1280	0.46
8.3	56	10	1510	0.58
8.3	91	10	2000	0.84
9.1	7	10	424	0.18
9.1	14	10	1050	0.51
9.1	28	10	863	0.41
9.1	56	10	1060	0.50
9.1	91	10	1420	0.69

Table A.14. Results of Static Tests on HIP Binder Glass in Buffer Solution at 20°C

pH	Duration (d)	S/V (m ⁻¹)	Concentration (µg Si/L)	NL (Si) (g/m ²)
4.8	7	10	105	-0.01
4.8	14	10	235	0.03
4.8	28	10	182	0.01
4.8	56	10	234	0.01
4.8	91	10	253	0.02
6.1	7	10	49	0.00
6.1	14	10	99	0.01
6.1	28	10	84	0.01
6.1	56	10	98	0.01
6.1	91	10	189	0.04
7.3	7	10	60	0.00
7.3	14	10	101	0.02
7.3	28	10	76	0.01
7.3	56	10	93	0.00
7.3	91	10	182	0.02
8.3	7	10	253	-0.02
8.3	14	10	677	0.08
8.3	28	10	702	0.09
8.3	56	10	696	0.09
8.3	91	10	1020	0.20
9.1	7	10	238	0.05
9.1	14	10	621	0.18
9.1	28	10	697	0.21
9.1	56	10	1220	0.37
9.1	91	10	1970	0.62

Table A.15. Results of Static Tests on HIP CWF in Buffer Solution at 20°C

pH	Duration (d)	S/V (m ⁻¹)	Concentration (µg Si/L)	NL (Si) (g/m ²)
4.8	7	10	14100	7.01
4.8	14	10	23400	11.68
4.8	28	10	32900	16.45
4.8	56	10	38700	19.35
4.8	91	10	43300	21.66
6.1	7	10	287	0.11
6.1	14	10	541	0.24
6.1	28	10	626	0.28
6.1	56	10	1480	0.71
6.1	91	10	2290	1.12
7.3	7	10	173	0.05
7.3	14	10	292	0.11
7.3	28	10	226	0.08
7.3	56	10	365	0.13
7.3	91	10	523	0.21
8.3	7	10	481	0.03
8.3	14	10	1110	0.34
8.3	28	10	980	0.28
8.3	56	10	1410	0.49
8.3	91	10	1910	0.75
9.1	7	10	585	0.25
9.1	14	10	982	0.45
9.1	28	10	746	0.33
9.1	56	10	1170	0.52
9.1	91	10	1370	0.62

Table A.16. Results of Static Tests on PC Binder Glass in Buffer Solution at 70°C

pH	Duration (d)	S/V (m ⁻¹)	Concentration (µg Si/L)	NL (Si) (g/m ²)
6.2	2	10	2460	1.22
6.2	3	10	4290	2.14
6.2	5	10	5890	2.94
6.2	7	10	7720	3.86
6.2	10	10	8700	4.36
8.2	2	10	1910	0.88
8.2	3	10	3500	1.68
8.2	5	10	4840	2.36
8.2	7	10	5210	2.54
8.2	10	10	5980	2.93
9.5	2	10	3090	1.53
9.5	3	10	5270	2.63
9.5	5	10	5610	2.80
9.5	7	10	7770	3.88
9.5	10	10	10400	5.19

Table A.17. Results of Static Tests on PC CWF in Buffer Solution at 70°C

pH	Duration (d)	S/V (m ⁻¹)	Concentration (□g Si/L)	NL (Si) (g/m ²)
6.2	2	10	258	0.07
6.2	3	10	340	0.10
6.2	5	10	534	0.17
6.2	7	10	462	0.14
6.2	10	10	822	0.27
8.2	2	10	2570	0.82
8.2	3	10	3610	1.17
8.2	5	10	4850	1.59
8.2	7	10	5680	1.87
8.2	10	10	7100	2.35
9.5	2	10	6040	2.03
9.5	3	10	6540	2.20
9.5	5	10	8440	2.85
9.5	7	10	11400	3.85
9.5	10	10	13400	4.52

Table A.18. Results of Static Tests on Modified Glass in Buffer Solution at 70°C

pH	Duration (d)	S/V (m ⁻¹)	Concentration (µg Si/L)	NL (Si) (g/m ²)
6.2	2	10	140	0.04
6.2	3	10	179	0.05
6.2	5	10	208	0.06
6.2	7	10	199	0.06
6.2	10	10	258	0.09
8.2	2	10	1390	0.44
8.2	3	10	1750	0.57
8.2	5	10	1910	0.63
8.2	7	10	2820	0.95
8.2	10	10	3750	1.28
9.5	2	10	3310	1.17
9.5	3	10	4130	1.46
9.5	5	10	5830	2.07
9.5	7	10	7100	2.52
9.5	10	10	8050	2.85

Table A.19. Results of Static Tests on CSG Glass in Buffer Solution at 70°C

pH	Duration (d)	S/V (m ⁻¹)	Concentration (i) (µg /L)				NL (i) (g/m ²)			
			Si	Al	Na	Ca	Si	Al	Na	Ca
6.2	2	10	209	30	1190	479	0.06	0.05	2.24	3.48
6.2	3	10	310	38.9	1700	664	0.09	0.07	3.29	5.37
6.2	5	10	304	41.4	1790	646	0.09	0.08	3.48	5.19
6.2	7	10	442	77.3	2630	961	0.14	0.17	5.22	8.42
6.2	10	10	480	63.3	2960	1050	0.16	0.14	5.99	9.33
7.3	2	10	284	15.9	719	298	0.06	0.01	0.61	0.20
7.3	3	10	327	30.6	773	333	0.07	0.02	0.66	0.28
7.3	5	10	393	37.4	1060	288	0.10	0.04	0.92	0.18
7.3	7	10	609	67.1	1260	490	0.18	0.12	1.10	0.60
7.3	10	10	639	85.3	1390	397	0.19	0.16	1.22	0.41
8.2	2	10	1490	252	804	672	0.45	0.54	1.22	5.46
8.2	3	10	2430	378	1300	669	0.77	0.86	2.25	5.43
8.2	5	10	3040	475	1650	811	0.98	1.11	2.98	6.88
8.2	7	10	3860	599	2020	1020	1.26	1.42	3.74	9.03
8.2	10	10	4950	769	2600	1370	1.62	1.84	5.11	12.62
9.5	2	10	5670	882	3030	1200	1.91	0.57	5.96	10.87
9.5	3	10	8230	1260	4410	1710	2.78	1.53	8.82	16.10
9.5	5	10	10500	1580	5780	2090	3.55	2.34	11.66	20.00
9.5	7	10	13400	2040	7210	2670	4.53	3.50	14.62	25.95
9.5	10	10	17400	2570	9350	3340	5.88	6.39	19.17	32.82

Table A.20. Results of Static Tests on CSG Glass with Three S/V Ratios at pH 9.4 Buffer Solution and 70°C

S/V, m ⁻¹	Duration (d)	Concentration (i) (µg /L)				NL (i) (g/m ²)			
		Si	Al	Na	Ca	Si	Al	Na	Ca
2.5	1	2450	492	1610	338	3.44	4.74	5.33	1.91
	2	2370	789	1310	502	3.31	7.78	4.24	3.24
	3	3310	511	1800	686	4.76	5.02	6.12	4.84
	4	3960	582	2070	823	5.61	5.65	6.97	5.86
	5	4710	700	2530	976	6.68	6.85	8.62	7.10
5	1	2180	1100	1130	412	1.52	5.07	1.81	1.25
	2	4330	870	2330	923	3.07	3.89	3.97	3.34
	3	6460	1050	3530	1350	4.61	4.82	6.14	5.08
	4	6270	1510	3380	1250	4.47	7.17	5.86	4.67
	5	6940	1560	3740	1410	4.96	7.43	6.51	5.33
10	1	2180	648	2060	861	0.75	1.19	1.74	1.54
	2	4330	1000	3580	1400	1.53	2.10	3.11	2.64
	3	6460	1440	4980	1930	2.30	3.22	4.37	3.73
	4	6270	1500	5450	2230	2.23	3.38	4.79	4.34
	5	6940	1460	5040	2140	2.47	3.27	4.42	4.15

Table A.21. Results of SPFT Tests in pH 6.2 Buffer at Different Nominal F/S°

Aliquot No.	F/S°, m/s	C(Si), ppm	NR, g/(m ² •d)	F/S°, m/s	C(Si), ppm	NR, g/(m ² •d)
	Series 1			Series 4		
1	3.31 x 10 ⁻⁶	0.0665	0.0732	9.97 x 10 ⁻⁸	0.428	0.0142
2	3.29 x 10 ⁻⁶	0.0755	0.0824	9.91 x 10 ⁻⁸	0.329	0.0108
3	3.27 x 10 ⁻⁶	0.0695	0.0755	9.93 x 10 ⁻⁸	0.272	0.0090
4	3.26 x 10 ⁻⁶	0.0655	0.0710	9.91 x 10 ⁻⁸	0.266	0.0087
5	3.25 x 10 ⁻⁶	0.0645	0.0697	9.87 x 10 ⁻⁸	0.275	0.0090
6	3.27 x 10 ⁻⁶	0.0515	0.0560	9.56 x 10 ⁻⁸	0.271	0.0086
7	3.26 x 10 ⁻⁶	0.0675	0.0730	8.93 x 10 ⁻⁸	0.270	0.0080
	Series 2			Series 5		
1	1.86 x 10 ⁻⁶	0.0955	0.0590	4.60 x 10 ⁻⁸	1.30	0.0199
2	1.71 x 10 ⁻⁶	0.0955	0.0542	4.57 x 10 ⁻⁸	0.850	0.0129
3	1.83 x 10 ⁻⁶	0.0995	0.0607	4.58 x 10 ⁻⁸	0.746	0.0114
4	1.84 x 10 ⁻⁶	0.0705	0.0432	4.58 x 10 ⁻⁸	0.604	0.0092
5	1.83 x 10 ⁻⁶	0.0655	0.0399	4.58 x 10 ⁻⁸	0.602	0.0092
6	1.85 x 10 ⁻⁶	0.0545	0.0335	4.51 x 10 ⁻⁸	0.534	0.0080
7	1.83 x 10 ⁻⁶	0.0585	0.0356	4.46 x 10 ⁻⁸	0.551	0.0082
	Series 3			Series 6		
1	4.03 x 10 ⁻⁶	0.153	0.0204	2.90 x 10 ⁻⁸	3.30	0.0318
2	4.01 x 10 ⁻⁶	0.121	0.0160	2.90 x 10 ⁻⁸	2.07	0.0200
3	4.02 x 10 ⁻⁶	0.111	0.0147	2.90 x 10 ⁻⁸	1.50	0.0145
4	4.00 x 10 ⁻⁶	0.109	0.0144	2.89 x 10 ⁻⁸	1.34	0.0129
5	3.95 x 10 ⁻⁶	0.110	0.0144	2.89 x 10 ⁻⁸	1.12	0.0108
6	4.03 x 10 ⁻⁶	0.0915	0.0123	2.84 x 10 ⁻⁸	1.00	0.0095
7	4.00 x 10 ⁻⁶	0.0975	0.0129	2.87 x 10 ⁻⁸	0.888	0.0085

Table A.22. Results of SPFT Tests in pH 7.3 Buffer at Different Nominal F/S°

Aliquot No.	F/S°, m/s	C(Si), ppm	NR, g/(m ² •d)	F/S°, m/s	C(Si), ppm	NR, g/(m ² •d)
	Series 1			Series 4		
1	6.53 x 10 ⁻⁷	0.161	0.0349	4.44 x 10 ⁻⁸	2.73	0.0402
2	6.64 x 10 ⁻⁷	0.093	0.0205	4.24 x 10 ⁻⁸	3.58	0.0504
3	6.48 x 10 ⁻⁷	0.079	0.0170	4.26 x 10 ⁻⁸	1.78	0.0252
4	6.53 x 10 ⁻⁷	0.073	0.0158	4.76 x 10 ⁻⁸	1.58	0.0250
5	6.64 x 10 ⁻⁷	0.070	0.0154	4.37 x 10 ⁻⁸	1.74	0.0253
6	6.64 x 10 ⁻⁷	0.069	0.0152	4.37 x 10 ⁻⁸	1.58	0.0229
7	6.48 x 10 ⁻⁷	0.077	0.0166	4.22 x 10 ⁻⁸	1.53	0.0215
8	6.56 x 10 ⁻⁷	0.061	0.0133	4.37 x 10 ⁻⁸	1.70	0.0247
	Series 2			Series 5		
1	4.25 x 10 ⁻⁷	0.361	0.123	2.99 x 10 ⁻⁸	3.53	0.0351
2	4.18 x 10 ⁻⁷	0.204	0.0359	2.87 x 10 ⁻⁸	2.51	0.0239
3	4.18 x 10 ⁻⁷	0.162	0.0278	2.92 x 10 ⁻⁸	2.11	0.0205
4	4.25 x 10 ⁻⁷	0.131	0.0233	3.05 x 10 ⁻⁸	1.97	0.0200
5	4.31 x 10 ⁻⁷	0.140	0.0239	3.14 x 10 ⁻⁸	1.87	0.0195
6	4.31 x 10 ⁻⁷	0.135	0.0254	3.16 x 10 ⁻⁸	1.96	0.0206
7	4.25 x 10 ⁻⁷	0.138	0.0241	3.11 x 10 ⁻⁸	1.88	0.0194
8	4.27 x 10 ⁻⁷	0.128	0.0238	3.09 x 10 ⁻⁸	1.95	0.0200
	Series 3			Series 6		
1	9.82 x 10 ⁻⁸	3.78	0.123	2.92 x 10 ⁻⁸	3.81	0.0369
2	9.48 x 10 ⁻⁸	1.140	0.0359	2.64 x 10 ⁻⁸	2.80	0.0245
3	9.83 x 10 ⁻⁸	0.850	0.0278	2.81 x 10 ⁻⁸	2.38	0.0222
4	9.72 x 10 ⁻⁸	0.720	0.0233	2.85 x 10 ⁻⁸	2.19	0.0207
5	9.91 x 10 ⁻⁸	0.725	0.0239	2.90 x 10 ⁻⁸	2.05	0.0197
6	9.82 x 10 ⁻⁸	0.779	0.0254	2.95 x 10 ⁻⁸	2.12	0.0208
7	9.70 x 10 ⁻⁸	0.747	0.0241	2.91 x 10 ⁻⁸	2.14	0.0207
8	9.82 x 10 ⁻⁸	0.730	0.0238	2.92 x 10 ⁻⁸	2.17	0.0210

Table A.23. Results of SPFT Tests in pH 8.2 Buffer at Different Nominal F/S°

Aliquot No.	F/S°, m/s	C(Si), ppm	NR, g/(m ² •d)	F/S°, m/s	C(Si), ppm	NR, g/(m ² •d)
	Series 1			Series 4		
1	3.30 x 10 ⁻⁶	0.502	0.552	9.77 x 10 ⁻⁸	5.47	0.178
2	3.30 x 10 ⁻⁶	0.547	0.600	9.79 x 10 ⁻⁸	4.88	0.159
3	3.28 x 10 ⁻⁶	0.465	0.507	9.80 x 10 ⁻⁸	5.43	0.177
4	3.27 x 10 ⁻⁶	0.447	0.486	9.46 x 10 ⁻⁸	5.21	0.164
5	3.27 x 10 ⁻⁶	0.384	0.417	9.74 x 10 ⁻⁸	5.31	0.172
6	3.29 x 10 ⁻⁶	0.369	0.403	9.98 x 10 ⁻⁸	4.52	0.150
7	3.29 x 10 ⁻⁶	0.444	0.485	9.83 x 10 ⁻⁸	4.27	0.140
8	3.29 x 10 ⁻⁶	0.339	0.371	9.81 x 10 ⁻⁸	4.70	0.153
	Series 2			Series 5		
1	1.87 x 10 ⁻⁶	0.580	0.361	4.17 x 10 ⁻⁸	8.65	0.120
2	1.87 x 10 ⁻⁶	0.541	0.337	4.26 x 10 ⁻⁸	8.25	0.117
3	1.86 x 10 ⁻⁶	0.554	0.342	4.31 x 10 ⁻⁸	8.51	0.122
4	1.84 x 10 ⁻⁶	0.553	0.339	4.45 x 10 ⁻⁸	8.10	0.120
5	1.87 x 10 ⁻⁶	0.580	0.360	4.40 x 10 ⁻⁸	7.99	0.117
6	1.85 x 10 ⁻⁶	0.511	0.315	4.62 x 10 ⁻⁸	7.84	0.121
7	1.87 x 10 ⁻⁶	0.531	0.329	4.47 x 10 ⁻⁸	7.74	0.115
8	1.86 x 10 ⁻⁶	0.546	0.338	4.44 x 10 ⁻⁸	7.59	0.112
	Series 3			Series 6		
1	4.05 x 10 ⁻⁷	1.75	0.236	2.73 x 10 ⁻⁸	10.0	0.091
2	4.03 x 10 ⁻⁷	1.69	0.226	2.86 x 10 ⁻⁸	10.1	0.096
3	4.01 x 10 ⁻⁷	1.81	0.241	2.86 x 10 ⁻⁸	9.82	0.093
4	3.97 x 10 ⁻⁷	1.68	0.222	2.80 x 10 ⁻⁸	9.40	0.088
5	4.02 x 10 ⁻⁷	1.80	0.240	2.86 x 10 ⁻⁸	10.6	0.101
6	4.02 x 10 ⁻⁷	1.61	0.215	2.89 x 10 ⁻⁸	10.1	0.098
7	4.03 x 10 ⁻⁷	1.65	0.221	2.89 x 10 ⁻⁸	10.3	0.099
8	4.02 x 10 ⁻⁷	1.59	0.212	2.87 x 10 ⁻⁸	9.70	0.0926

Table A.24. Results of SPFT Tests in pH 9.5 Buffer at Different Nominal F/S°

Aliquot No.	F/S°, m/s	C(Si), ppm	NR, g/(m ² •d)	F/S°, m/s	C(Si), ppm	NR, g/(m ² •d)
	Series 1			Series 5		
1	7.07 x 10 ⁻⁶	0.607	1.42	8.35 x 10 ⁻⁸	18.5	0.514
2	6.89 x 10 ⁻⁶	0.509	1.16	8.28 x 10 ⁻⁸	18.0	0.496
3	7.12 x 10 ⁻⁶	0.686	1.62	8.34 x 10 ⁻⁸	17.6	0.489
4	6.95 x 10 ⁻⁶	0.627	1.44	8.37 x 10 ⁻⁸	21.4	0.596
5	6.99 x 10 ⁻⁶	0.529	1.23	8.37 x 10 ⁻⁸	18.1	0.504
6	7.11 x 10 ⁻⁶	0.481	1.13	8.69 x 10 ⁻⁸	17.7	0.512
7	6.99 x 10 ⁻⁶	0.591	1.37	8.73 x 10 ⁻⁸	17.4	0.506
8	7.03 x 10 ⁻⁶	0.575	1.34	8.71 x 10 ⁻⁸	18.5	0.537
9	7.03 x 10 ⁻⁶	0.569	1.33	8.76 x 10 ⁻⁸	18.6	0.543
10	6.99 x 10 ⁻⁶	0.595	1.38	8.71 x 10 ⁻⁸	19.2	0.557
	Series 2			Series 6		
1	3.31 x 10 ⁻⁶	1.78	1.96	4.46 x 10 ⁻⁸	22.9	0.340
2	3.30 x 10 ⁻⁶	2.51	2.76	4.38 x 10 ⁻⁸	21.3	0.311
3	3.34 x 10 ⁻⁶	1.57	1.75	4.41 x 10 ⁻⁸	21.5	0.315
4	3.31 x 10 ⁻⁶	1.85	2.04	4.36 x 10 ⁻⁸	23.2	0.337
5	3.27 x 10 ⁻⁶	1.88	2.05	4.34 x 10 ⁻⁸	22.8	0.330
6	3.30 x 10 ⁻⁶	1.75	1.92	4.53 x 10 ⁻⁸	23.5	0.354
7	3.29 x 10 ⁻⁶	1.68	1.84	4.54 x 10 ⁻⁸	22.9	0.346
8	3.29 x 10 ⁻⁶	1.75	1.92	4.50 x 10 ⁻⁸	23.8	0.356
9	3.28 x 10 ⁻⁶	1.59	1.74	4.53 x 10 ⁻⁸	23.3	0.351
10	3.29 x 10 ⁻⁶	1.79	1.96	4.49 x 10 ⁻⁸	23.2	0.347
	Series 3			Series 7		
1	1.86 x 10 ⁻⁶	3.04	1.89	2.94 x 10 ⁻⁸	23.9	0.234
2	1.86 x 10 ⁻⁶	2.88	1.78	2.81 x 10 ⁻⁸	23.2	0.217
3	1.84 x 10 ⁻⁶	2.58	1.58	2.92 x 10 ⁻⁸	23.4	0.227
4	1.84 x 10 ⁻⁶	2.97	1.82	2.87 x 10 ⁻⁸	23.9	0.229
5	1.84 x 10 ⁻⁶	2.96	1.81	2.94 x 10 ⁻⁸	24.7	0.242
6	1.85 x 10 ⁻⁶	2.96	1.82	2.98 x 10 ⁻⁸	23.2	0.230
7	1.85 x 10 ⁻⁶	2.80	1.72	3.00 x 10 ⁻⁸	23.9	0.239
8	1.85 x 10 ⁻⁶	2.65	1.63	2.92 x 10 ⁻⁸	25.0	0.243
9	1.84 x 10 ⁻⁶	2.84	1.74	2.98 x 10 ⁻⁸	25.1	0.249
10	1.85 x 10 ⁻⁶	2.81	1.73	2.98 x 10 ⁻⁸	24.7	0.245
	Series 4					
1	4.03 x 10 ⁻⁷	9.39	1.26			
2	4.02 x 10 ⁻⁷	8.83	1.18			
3	4.05 x 10 ⁻⁷	8.70	1.17			
4	4.03 x 10 ⁻⁷	8.32	1.11			
5	4.01 x 10 ⁻⁷	8.59	1.15			
6	4.01 x 10 ⁻⁷	8.26	1.10			
7	4.00 x 10 ⁻⁷	8.38	1.12			
8	3.98 x 10 ⁻⁷	8.63	1.14			
9	3.95 x 10 ⁻⁷	7.60	1.00			
10	3.96 x 10 ⁻⁷	8.08	1.06			

Table A.25. Steady-State Si Concentrations and Dissolution Rates

Series	F/S°, m/s	C ^{ss} (Si), ppm	NR, g/(m ² •d)
pH 6.2			
1	3.26 x 10 ⁻⁶	0.0623	0.0674
2	1.84 x 10 ⁻⁶	0.0623	0.0380
3	3.99 x 10 ⁻⁷	0.102	0.0135
4	9.57 x 10 ⁻⁸	0.270	0.00859
5	4.53 x 10 ⁻⁸	0.572	0.00862
6	2.87 x 10 ⁻⁸	1.09	0.0104
pH 7.3			
1	6.58 x 10 ⁻⁷	0.0693	0.0151
2	4.28 x 10 ⁻⁷	0.135	0.0193
3	9.81 x 10 ⁻⁸	0.745	0.0243
4	4.33 x 10 ⁻⁸	1.64	0.0236
5	3.12 x 10 ⁻⁸	1.92	0.0199
6	2.92 x 10 ⁻⁸	2.12	0.0206
pH 8.2			
1	3.28 x 10 ⁻⁶	0.397	0.432
2	1.86 x 10 ⁻⁶	0.544	0.336
3	4.01 x 10 ⁻⁷	1.67	0.222
4	9.76 x 10 ⁻⁸	4.80	0.156
5	4.48 x 10 ⁻⁸	7.85	0.117
6	2.86 x 10 ⁻⁸	10.0	0.0956
pH 9.5			
1	7.03 x 10 ⁻⁶	0.562	1.31
2	3.29 x 10 ⁻⁶	1.72	1.88
3	1.85 x 10 ⁻⁶	2.82	1.73
4	3.98 x 10 ⁻⁷	8.19	1.08
5	8.72 x 10 ⁻⁸	18.3	0.531
6	4.52 x 10 ⁻⁸	23.4	0.351
7	2.97 x 10 ⁻⁸	24.4	0.241

Distribution for ANL-02/32

Internal (Printed and Electronic Copies):

W. L. Ebert (25)
T. H. Fanning

K. M. Goff (3)
S-Y. Jeong

M. A. Lewis

Internal (Printed Copy Only):

V. A. Davis
S. K. Zussman

Internal (Electronic Copy Only):

M. R. Hale, TIS
J. P. Ackerman
C. H. Adams
R. K. Ahluwalia
S. E. Aumeier
A. J. Bakel
T. L. Barber
K. J. Bateman
T. J. Battisti
T. H. Bauer
R. W. Benedict
A. R. Brunsvold
D. B. Chamberlain
Y. I. Chang
J. C. Cunnane
S. S. Cunningham
D. B. Davies
N. L. Dietz
R. N. Elliot
R. A. Evans
R. J. Finch
J. K. Fink
J. A. Fortner

E. K. Fujita
H. E. Garcia
E. Gay
M. M. Goldberg
M. G. Gougar
C. Grandy
D. J. Graziano
D. D. Hagan
J. E. Herceg
S. G. Johnson
D. D. Keiser, Jr.
J. R. Kennedy
C. J. Knight
J. R. Krsul
C. E. Lahm
R.M. Lell
G. L. Lentz
D. Lewis
S. X. Li
R. P. Lind
D. Lexa
K. C. Marsden
S. D. McBride

S. M. McDeavitt
H. F. McFarlane
L. Nuñez
T. P. O'Holleran
R. L. Parks
D. R. Pedersen
R. D. Phipps
C. L. Pope
M. C. Regalbutto
R. H. Rigg
S. R. Sherman
M. F. Simpson
G. M. Teske
K. L. Toews
Y. Tsai
D. Vaden
G. F. Vandegrift
D. L. Wahlquist
B. R. Westphal
R. A. Wigeland
M. A. Williamson
J. L. Willit
T. L. Wright

External (Printed Copy Only):

L. R. Morss, USDOE, Germantown, MD

External (Electronic Copy Only):

M. A. Buckley, ANL-E Library

E. Sackett, ANL-W Library

Chemical Technology Review Committee Members:

H. U. Anderson, University of Missouri-Rolla, Rolla, MO

R. A. Greenkorn, Purdue University, West Lafayette, IN

C. L. Hussey, University of Mississippi, Oxford, MS

M. Koch, University of Washington, Seattle, WA

V. Roan, Jr., University of Florida, Gainesville, FL

J. R. Selman, Illinois Institute of Technology, Chicago, IL

J. S. Tulenko, University of Florida, Gainesville, FL